# **Comprehensive Dynamics in a Polyelectrolyte Complex Coacervate**

Khalil Akkaoui, Zachary A. Digby, Changwoo Do, Joseph B. Schlenoff\*

Department of Chemistry and Biochemistry

The Florida State University, Tallahassee, FL 32306 U.S.A.

Neutron Scattering Division, Oak Ridge National Laboratory, Oak Ridge, TN 37831

**Keywords**: liquid-liquid phase separation; doping; saloplastic; charge pairing; viscoelasticity; condensate; salt; SANS.

\*jschlenoff@fsu.edu

# **Abstract**

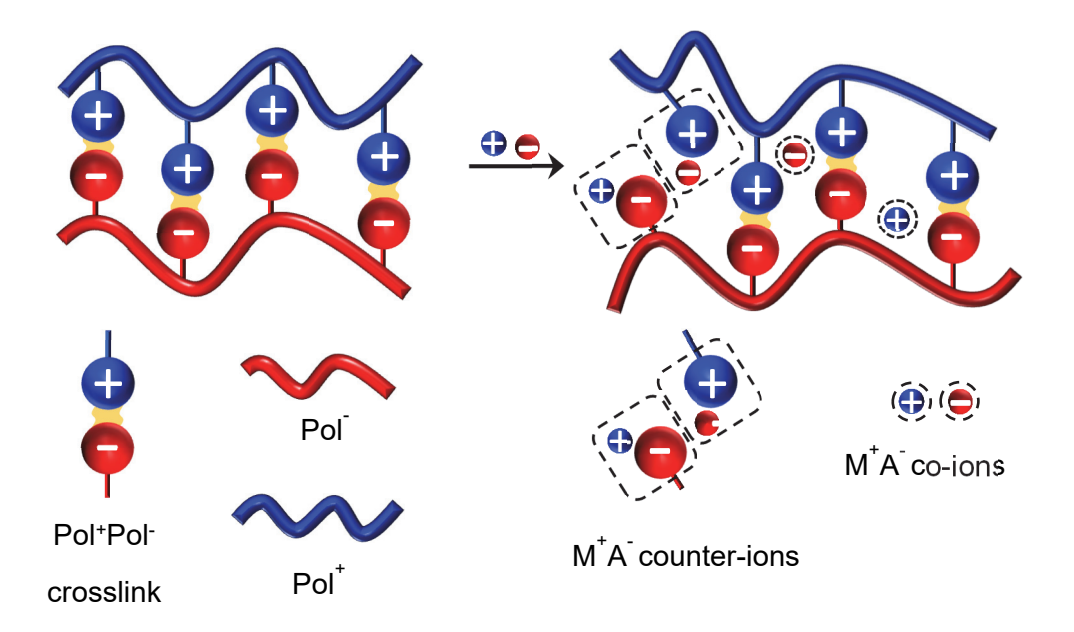
The linear viscoelastic response, LVR, of a hydrated polyelectrolyte complex coacervate, PEC, was evaluated over a range of frequencies, temperatures, and salt concentrations. The PEC was nearly-stoichiometric blend quaternary of ammonium -61)vloa (methacrylamido)propyl]trimethylammonium chloride), PMAPTAC, and poly(2-acrylamido-2methyl-1-propanesulfonic acid sodium salt), PAMPS, an aliphatic sulfonate, selected because they remain fully charged over the conditions of use. Narrow molecular weight distribution polyelectrolytes were prepared using fractionation techniques. A partially deuterated version of PMAPTAC was incorporated to determine the coil radius of gyration, R<sub>g</sub>, within PECs using small angle neutron scattering. Chain dimensions were determined to be Gaussian with a Kuhn length of 2.37 nm, which remained constant from 25 to 65 °C. The LVR for a series of matched molecular weight PECs, mostly above the entanglement threshold, exhibited crossovers of modulus versus frequency classically attributed to the reptation time, relaxation between entanglements, and the relaxation of a Kuhn length of units (the "monomer" time). The scaling for zero shear viscosity,  $\eta_0$ , versus chain length N, was  $\eta_0 \sim N^{3.1}$ , in agreement with "sticky reptation" theory. The lifetime and activation energy, Ep, of a pair between polyanion and polycation repeat units, Pol+Pol-, were determined from diffusion coefficients of salt ions within the PEC. The activation energy for LVR of salt-free PECs was 2E<sub>p</sub>, showing that the key mechanism limiting the dynamics of undoped PECs is pair exchange. An FTIR technique was used to distinguish whether SCN acts as a counterion or a co-ion within PECs. Doping of PECs with NaSCN breaks Pol+Pol- pairing efficiently, which decreases effective crosslinking and decreases viscosity. An equation was derived that quantitatively predicts this effect.

## Introduction

An intriguing soft material spontaneously phase separates when solutions of polyelectrolytes with opposite charges are mixed. When immersed in aqueous solutions, these polyelectrolyte complexes retain substantial amounts of water, yet they display properties ranging from glassy (below a well-defined glass transition temperature,  $T_g$ ), to rubbery/liquidlike above  $T_g$ . Complexes above their  $T_g$  at room temperature are usually termed "coacervates," a definition originating from the droplet-like morphologies of biopolymer complexes observed by Bungenberg de Jong and coworkers.<sup>2</sup> Here, the term PEC is used in its most general sense to mean polyelectrolyte complexes or coacervates.

Microscopic representations of PECs usually depict pairing of repeat units on the polycation, Pol<sup>+</sup>, and polyanion, Pol<sup>-</sup>, illustrated in Scheme 1, which shows a stoichiometric PEC with equal numbers of positive and negative repeat units. Pol<sup>+</sup>Pol<sup>-</sup> charge pairs that have appreciable lifetimes can be considered to be physical crosslinks.

**Scheme 1**. Depiction of a stoichiometric PEC showing Pol<sup>+</sup>Pol<sup>-</sup> charge pairings, also known as "intrinsic sites," and Pol<sup>+</sup>A<sup>-</sup> and Pol<sup>-</sup>M<sup>+</sup>, extrinsic sites (within dotted squares), where salt MA acts as counterions. Some salt ions within the PEC exist as coions (highlighted by dotted circles).



The crosslink is a fundamental construct in macromolecular science. If permanent, crosslinks make glassy materials stiffer, or they turn liquid-like polymers into rubbery ones.<sup>3</sup> There has been intense interest in dynamic crosslinks, which may be chemical or physical in nature.<sup>4-5</sup> The latter category includes hydrogen bonding <sup>6</sup> and "electrostatic" interactions such as those represented in Scheme 1.

The addition of salt, M<sup>+</sup>A<sup>-</sup>, introduces a processing dimension not available to neutral polymers: as more salt is added to solution it enters the PEC and breaks interactions between polymers.<sup>7</sup> This effective decrease in crosslink density makes the PEC more fluidlike. Added salt transforms a glassy polymer into a rubbery one, enabling processing such as extrusion,<sup>8</sup> spin coating,<sup>9</sup> bar coating,<sup>10</sup> embossing,<sup>11</sup> compression,<sup>7, 12</sup> and electrospinning.<sup>13</sup> This "saloplasticity" promotes self-healing driven by enhanced chain mobility at intermediate salt concentrations.<sup>7</sup>

Salt effects on polyelectrolyte solution conformations and properties are usually explained using continuum electrostatics arguments, wherein salt "shields" Coulombic interactions between charges. A similar mechanism is often used to explain the control of Pol+Pol- interactions in PECs by MA. An alternative approach focuses on a site-specific interplay between paired or unpaired units, connected via chemical equilibria. Electrostatic theories take a step towards site-specificity by introducing charge-charge correlations.

In the ideal specific salt "doping" model, one MA breaks one crosslink, illustrated in Scheme 1. In fact, not all MA that enters a PEC breaks  $Pol^+Pol^-$  pairs (Scheme 1). Those that do so are termed counter-ions and those that do not are co-ions.<sup>23</sup> Though incorporated into theory,<sup>24</sup> to this point it has proven difficult to measure the fraction f of MA within the PEC acting as counterions. If f =1, all salt within a PEC breaks charge pairs and the influence of physical crosslinking density on PEC properties such as linear viscoelastic response, LVR, could be reliably modeled.

Viscoelastic measurements of PECs yield critical information on the dynamics of these amorphous, hydrated materials.<sup>17, 25-30</sup> Variables such as frequency and temperature, available to rheology, may be used to investigate modulus and viscosity as a function of molecular weight, and molecular weight distribution.<sup>31</sup> Many PECs exist in near-equilibrium with the "dilute phase" in which they are immersed and salt concentration is a reproducible and reversible variable.

The effects on phase compositions and LVR by reversibly breaking Pol<sup>+</sup>Pol<sup>-</sup> pairs using salt have been studied intensively over the last decade.<sup>26, 32-36</sup> Polyelectrolyte pairs with matched molecular weights are optimal for studying chain relaxation dynamics. LVR for polymers exceeding the entanglement molecular weight, M<sub>c</sub>, may be compared to theories for "sticky reptation," which account for transient interactions between "sticker" groups.<sup>37-39</sup>

We have studied LVR for PECs below and above  $M_c$  using poly(methacrylic acid) salts, PMA, and poly([3-(methacrylamido)propyl]trimethylammonium chloride), PMAPTAC.<sup>40</sup> This pair forms a liquidlike PEC, far above  $T_g$  at room temperature, which behaves like a polymer melt. Using carefully fractionated materials, time-temperature superposition produced LVR that was broad enough to show several classical crossovers in storage and loss modulus (G' and G'' respectively) as a function of frequency. This work illustrated strong slowing of polymer dynamics on all scales but produced the unusual result that zero-shear viscosity,  $\eta_o$ , scaled as  $N^5$  rather than  $N^3$  (predicted by theory).<sup>37, 40</sup> Subsequent studies of PECs containing pH-sensitive (also termed "weak") polyelectrolytes revealed a complex interplay between salt concentration, pH and the degree of association and protonation within the PEC:<sup>41</sup> the presence of an oppositely-charged polymer, or salt, shifts the apparent  $pK_a^{42}$  which shifts the Pol\*Pol- density.<sup>43</sup> Narrow molecular weight distribution polypeptides have been employed for many PEC systems.<sup>33, 36, 44</sup> However, there is a wide range of LVR responses attributed to the hydrogen bonding programmed into these biopolymers.<sup>45-46</sup>

Given the intense interest in PEC composition and dynamics, a good representative system is needed. The goals of the present work were to establish reliable LVR in a strongly charged, synthetic, liquidlike, entangled PEC, free of hydrogen bonding and made with narrow molecular weight distribution components. Comparison to theory places several additional demands on the system: first, PECs must be stoichiometric. Second, the chain dimensions and the "ideal monomer" Kuhn length, and whether this changes with temperature, must be measured. In addition, the mechanism for relaxation at the monomer length scale must be established. Finally, when salt is added to PECs the fraction *f* that breaks charge pairs must be known so that the effective sticker density can be calculated.

# **Experimental Section**

**Materials.** [3-(Methacryloylamido)propyl]trimethylammonium chloride (MAPTAC, 50 wt. % in  $H_2O$ ), 2-acrylamido-2-methyl-1-propanesulfonic acid sodium salt (AMPS, 50 wt. % in  $H_2O$ ), N-(3-aminopropyl)methacrylamide hydrochloride (AMA), dimethyl formamide (DMF),  $d_3$ -iodomethane (CD $_3$ I), ethyl acetate, 1,2,2,6,6-pentamethylpiperidine (PMP), inhibitor removal beads, sodium nitrate (NaNO $_3$ ), sodium azide (NaN $_3$ ), and sodium thiocyanate (NaSCN) were from Sigma Aldrich. Acetone used for fractionation and polymer purification was from Fisher Chemicals. Deuterium dioxide (D $_2O$ , 99.9%) was from Cambridge Isotope laboratories. The radioactive salts

were sodium chloride ( $^{22}$ NaCl, 54.3  $\mu$ Ci) from Perkin Elmer and potassium thiocyanate (KS $^{14}$ CN, 100  $\mu$ Ci) from ViTrax. Ultrapure water (18.2 M $\Omega$  cm) was supplied via a Barnstead E-Pure system (Thermo Scientific) to prepare all solutions.

**Polymer Synthesis**. Solutions of MAPTAC and AMPS monomers were stirred for 4 h with inhibitor removal beads. After filtering out the beads, 50 mL of MAPTAC solution was diluted with water to a concentration of 1.19 M. A similar dilution with AMPS yielded 1.46 M AMPS. 8 mg  $K_2S_2O_8$  initiator was added to the solutions and free radical polymerization was carried out at 65 °C under  $N_2$  and stirring for 18 h. The polymer solutions were freeze dried then dried at 120 °C for 18 h.

**Polyelectrolyte Fractionation**. To isolate polyelectrolyte (PE) samples with low dispersity, molecular weight fractionation was carried out with the starting PMAPTAC ( $M_w = 311 \text{ kg mol}^{-1}$ , D = 2.32) and PAMPS ( $M_w = 119 \text{ kg mol}^{-1}$ , D = 1.71) samples. Acetone was gradually added to 10 g of PMAPTAC or PAMPS in 100 mL water. Each fraction precipitating out was collected by centrifuging the solution at 6000 rpm for 30 - 60 min. Additional acetone was added to the remaining polymer solution and the process repeated to obtain several fractions. The fractions were dried at 120 °C for 18 h. Unless otherwise stated, PMAPTA/PAMPS PECs were made with the D = 2.32/1.71 mentioned above.

Size Exclusion Chromatography (SEC). Size exclusion chromatography (Supporting Information Figure S1) was used to determine the weight-average molecular weight,  $M_{\text{w}}$ , number-average molecular weight,  $M_{\text{n}}$ , and the dispersity index ( $\Phi = M_{\text{w}}/M_{\text{n}}$ ), all given in Table 1. Molecular weights include the counterions of the mobile phase (see Supporting Information for a detailed procedure).

**Table 1**.  $M_w$ ,  $M_n$ ,  $\Theta$  and n of the PMAPTA(NO<sub>3</sub>) and PAMPS fractions. n is the average number of monomers per polymer chain.  $n = M_n/M_0$ , and  $M_0$  the molecular weight of the monomer repeat unit: 247 g mol<sup>-1</sup> for MAPTA(NO<sub>3</sub>), and 229 g mol<sup>-1</sup> for AMPSNa and N the number of Kuhn segments

	<b>M</b> w kg	Mn			N
	mol <sup>-1</sup>	kg mol <sup>-1</sup>	Đ	n	
PMAPTA(NO <sub>3</sub> )	39.5	33.2	1.16	134	14
(~   }	181	168	1.09	679	72
O NH	217	190	1.14	769	82
	349	319	1.09	1290	137
NO <sub>3</sub> - N+	390	356	1.10	1440	153
	613	554	1.11	2241	238
PAMPS	54.6	51.3	1.06	224	24
f n	139	128	1.09	559	60
O NH	215	206	1.04	898	96
Na <sup>+ -</sup> O-S=O Ö	270	248	1.09	1085	115
	370	347	1.06	1517	161
	502	472	1.06	2063	219

**Preparing Stoichiometric Polyelectrolyte Complexes**. Nearly stoichiometric PECs were prepared by mixing equimolar solutions (0.125 M) of PMAPTAC and PAMPS in 0.1 M NaSCN. The mixture was stirred for an hour at room temp and the polymer rich phase (PEC) was collected. The PEC was rinsed in water to wash out the salt ions, then dried for 18 h at 120 °C. The ratio of PMAPTA:PAMPS was measured using NMR (Supporting Information Figure S2) and verified by radiolabeling (see below). For NMR, 10 mg of sample was dissolved in 1.0 mL, 1.0 M NaSCN in  $D_2O$  (for PMAPTAC or PAMPS homopolymers) while the complexes were dissolved in 0.6 M NaSCN in  $D_2O$ , and  $^1H$  NMR spectra were collected using an AVANCE 600 MHz NMR (Bruker). All PECs were liquidlike and transparent.

**Radiolabeling**. The degree of non-stoichiometry can be precisely measured by determining the amount of residual counter ions. Excess charge from either polyelectrolyte will be compensated by a counter-ion (Na<sup>+</sup> compensates *excess* AMPS<sup>-</sup> and SCN<sup>-</sup> compensates *excess* MAPTA<sup>+</sup>). Unlabeled counterions were replaced with labeled ones by soaking the PEC in a dilute solution of radiolabeled ions (NaS<sup>14</sup>CN or <sup>22</sup>NaSCN) as in prior work (see Supporting Information for detailed procedure). The number of moles of PEC, <sup>22</sup>Na<sup>+</sup> and S<sup>14</sup>CN<sup>-</sup> in the PEC are given in Table 2.

Table 2. Stoichiometry of P1479 PEC via radiolabeling

P1479 (mol repeat units)	1.52 x 10 <sup>-4</sup>
S <sup>14</sup> CN <sup>-</sup> PEC (mol)	3.27 x 10 <sup>-6</sup>
<sup>22</sup> Na⁺ PEC (mol)	5.12 x 10 <sup>-7</sup>
Pol+:Pol-	1.018

A small amount of salt enters the PEC via doping, which introduces *both* Na<sup>+</sup> and SCN<sup>-</sup>. Excess Pol<sup>+</sup> only brings in SCN<sup>-</sup> The stoichiometry is given by

$$\frac{[Pol^+]}{[Pol^-]} = 1 + \frac{molesSCN^- - molesNa^+}{molesPEC}$$
[1]

Critical Salt Concentration (CSC). Turbidimetry was used to determine the CSC. A Cary 100 UV-Visible spectrophotometer (Varian) was used to measure the absorbance of 1 mg mL<sup>-1</sup> solutions of PMAPTA/PAMPS at  $\lambda$  = 450 nm. 0.025 g of dry PEC was dissolved in 25 mL of 0.6 M NaSCN. Solutions with  $n_{avg}$  = 1188, 834 and 179 were prepared and their absorbances measured as the concentration of NaSCN was varied near the PEC CSC, which was determined to be between 0.5 and 0.6 M NaSCN by visual inspection of the point at which sufficient NaSCN had been added to dissolve the PEC. 2 mL of each dissolved PEC solution was diluted with aliquots of 100  $\mu$ L H<sub>2</sub>O until the absorbance increased to above 1 ("reverse" method). 100  $\mu$ L of [NaSCN] = 0.6 M was then gradually added to increase the concentration back to above the CSC ("forwards" method), until the solution no longer scattered light (absorbance  $\approx$  0).

**Doping Behavior.** The composition, including the concentration of salt in the PEC, [NaSCN]<sub>PEC</sub>, as a function of the concentration of salt in solution (dilute phase), [NaSCN]<sub>s</sub>, was determined by soaking a known mass of dry PMAPTA/PAMPS in different [NaSCN]<sub>s</sub> (0.3, 0.2, 0.1, 0.08, 0.06, 0.04, 0.02, 0.01 M), removing the supernatant, then releasing the PEC salt ions into 110 mL water in a jacketed, temperature controlled cell and recording the conductivity using a four-probe conductivity cell (Orion 013005MD, Thermo Scientific) and a conductivity meter (Orion 3 star, Thermo Scientific). The conductivity at long time,  $\sigma_{\infty}$ , assumed to correspond to release of all salt in the PEC, was converted to the salt content using conductivity standards. The water content was determined from the mass of the hydrated PEC in the various [NaSCN]<sub>s</sub>. The conductivity cell was thermostatted to  $\pm$  0.1 °C with a Thermo Haake K20 circulator and stirred with a large paddle.

**Linear Viscoelastic Response.** The storage modulus G', loss modulus, G'', and complex viscosity,  $\eta$ , for the PEC pairs were evaluated as a function of temperature and salt concentration using a stress-controlled DHR-3 rheometer (TA Instruments). PEC pairs P179, P619, P834, P1188, P1479, P2152, P1 and P2 (details given in Table 3) were soaked in 0.01M NaSCN for a minimum of 18 h, loaded onto the lower plate of the rheometer, and compressed using a 20 mm upper plate while immersed in 0.01 M NaSCN using a reservoir built in-house. The reservoir was equipped with a lid to prevent evaporation. The storage and loss modulus were recorded as a

function of oscillation frequency across a range of temperatures (between -5 and 85 °C) at 0.1% strain, well within the linear viscoelastic regime. Time-temperature superposition (TTS) was performed to obtain responses at a reference temperature  $T_r = 25$  °C across a wide range of effective frequencies ( $10^{-4} - 10^5$  rad s<sup>-1</sup>).

For zero shear viscosities, the steady state viscosity was recorded as a function of shear rate at 55 °C using the lowest range of shear rates available ( $10^{-4}$  - $10^{-2}$  rad s<sup>-1</sup>). The system was given 180 s to reach equilibrium after applying a shearing force. Viscosity independent of shear rate gave a plateau of values, which were averaged across the plateau to yield  $\eta_0$ , zero-shear viscosity, as a function of molecular weight and salt concentrations (for the pair  $n_{av}$  = 1479).

**Table 3**. Pairs of PMAPTA and PAMPS with matched, or mismatched, chain lengths. The average number of Kuhn segments (N<sub>av</sub>) in the PMAPTA/PAMPS pairs. Mole ratio of PMAPTA<sup>+</sup>:PAMPS<sup>-</sup> measured by NMR. P179 was below entanglement. P1 and P2 were mismatched lengths.

$P_{\text{nav}}$	$\mathbf{n}_{av}$	N <sup>+</sup>	N <sup>-</sup>	$N_{av}$	Pol <sup>+</sup> :Pol <sup>-</sup>
P179	179	14.3	23.8	19.1	0.97:1
P619	619	72.2	59.4	65.9	0.98:1
P834	834	81.8	95.5	88.7	0.98:1
P1188	1188	137	115	126	0.97:1
P1479	1479	153	161	157	0.99:1
P2152	2152	238	219	229	0.98:1
P1	-	239	24	-	0.96:1
P2	-	15	219	-	1:1.02

FTIR Spectroscopy. Attenuated total internal reflection Fourier transform infrared spectroscopy (ATR-FTIR) was used to monitor the absorbances corresponding to the C≡N stretch for thiocyanate (at 2060 cm⁻¹ when SCN⁻ is a counter ion and 2064 cm⁻¹ when it is a co₋ion). Spectra of 0.6 M aqueous NaSCN, 1.0 M PMAPTA⁺ with SCN⁻ as counterion (PMAPTA(SCN)), 1.0 M PAMPS dissolved in 0.6 M NaSCN, and PMAPTA/PAMPS PEC doped in 0.3 M NaSCN were collected at 0.5 cm⁻¹ resolution using a ThermoScientific Nicolet iS20 with a Pike MIRacle ATR attachment fitted with a single-reflection diamond/ZnSe crystal. The background for all measurements was air. PMAPTA(SCN) was obtained via ion exchange by dialyzing a dilute solution of PMAPTAC against NaSCN (see above).

**Measuring Ion Diffusion.** The diffusion coefficient,  $D_{ions}$  (cm<sup>2</sup> s<sup>-1</sup>), of NaSCN in PMAPTA/PAMPS was measured as a function of temperature using the kinetics of salt release from the PEC into a solution of fresh water over a temperature range of 5 to 65 °C. 1.43 g of hydrated PMAPTA/PAMPS soaked in 0.10 M NaSCN, 0.066 cm thickness, 2.5 cm radius, was placed inside a water jacketed beaker connected to a circulating thermostat. 110 mL water, equilibrated at the target temperature, was poured over the coacervate disk at t = 0 and the conductivity was recorded every 10 s until a plateau was reached. To ensure kinetics of salt release were limited by diffusion through the PEC, and not by diffusion through solution, the solution above the PEC was briskly stirred with a large paddle.

The tracer diffusion coefficient of SCN-,  $D_{SCN-}$ , within PECs doped with [NaSCN]<sub>s</sub> = 0.01, 0.02, 0.04, 0.08, 0.16 and 0.3 M was measured at room temperature (T = 23.4 °C) by self-exchange of labeled (S<sup>14</sup>CN-) with unlabeled SCN-. 0.15 g of dry PMAPTA/PAMPS was added to 10 mL of each salt concentration (starting with 0.01 M NaSCN) and 10  $\mu$ L of NaS<sup>14</sup>CN (1  $\mu$ Ci, 1 Ci = 3.7 x 10<sup>10</sup> disintegrations per second) was added. 24 h was allowed for the radioisotope to exchange into the PEC. The kinetics of SCN- release was measured by removing the radioactive solution and substituting it with an unlabeled NaSCN solution of the same concentration. Maintaining vigorous stirring, 100  $\mu$ L aliquots were extracted at different times, mixed with 2 mL liquid scintillation cocktail and the counts were recorded using the <sup>14</sup>C channel of the scintillation counter until the count rate of sequential aliquots reached a plateau.

**Small-Angle Neutron Scattering (SANS).** The syntheses of deuterated monomer and polymer are described in Supporting Information. The deuterated polymer was fractionated as above into samples with defined size and paired with a polyelectrolyte with matching degree of polymerization (Table 4, Figure S3, Table S1). A 1:4 mole ratio mixture of deuterated and non-deuterated PMAPTAC was complexed with PAMPS under stoichiometric conditions.

**Table 4**. n<sup>+</sup> the number of repeat units in PMAPTA<sup>+</sup>, n<sup>-</sup> the number of repeat units in PAMPS<sup>-</sup> and n<sup>D+</sup>, the number of repeat units in the deuterated PMAPTA<sup>+</sup> comprising the samples used in neutron diffraction.

Nondeuterated components were contrast matched using a 1:4  $D_2O:H_2O$  mixture. Scattering length densities (SLDs) of one PMAPTA/PAMPS unit ( $C_{17}H_{33}N_3O_sS$ ) at different  $D_2O:H_2O$  ratios were matched with the appropriate 0.1 M NaSCN  $D_2O:H_2O$  mixture of equal SLD. The SLDs were calculated using the NIST online calculator (density = 1.1 g cm<sup>-3</sup>, sample thickness = 1 mm, and neutron wavelength of 6 Å). PECs **d-A** and **d-B** were soaked in 0.1 M NaSCN/1:4  $D_2O:H_2O$  and annealed at 50 °C for 18 h. The complexes were then loaded into 1 mm path 20 mm diameter silica banjo cells, sealed while covered with the contrast matched solved and annealed at 45 °C for 3 days. The samples were slowly cooled back to room temperature. SANS measurements were performed on the extended q-range small-angle neutron scattering diffractometer (EQSANS) at the Spallation Neutron Source (SNS) at Oak Ridge National Laboratory (ORNL). Two

sample-to-detector distances (9m and 4m) in combination of wavelength bands defined by minimum wavelength of 15 Å and 2.5 Å, respectively, were used to cover the q-range of 0.003 Å  $^{-1} < q < 0.3^{-1}$ , where the magnitude of the scattering vector, q, is defined by  $q = (4\pi/\lambda)sin(\theta)$ . Here,  $\lambda$  is the wavelength of neutron and  $2\theta$  is the scattering angle. Absolute scale intensities were calibrated with a porous silica standard sample. Measurements were performed at 25 °C for samples d-A and d-B, and a reference banjo cell loaded with the contrast matched electrolyte. Sample d-B was also measured at 35, 45 and 65 °C. The data reduction including corrections for detector sensitivity and background was performed using MantidPlot software. SasView was used to fit the data to the scattering intensity versus q for a monodisperse Gaussian coil.

## Results

SANS was used to evaluate the radius of gyration,  $R_g$ , of D-PMAPTA in PMAPTA/PAMPS, and thence the length of a statistical Kuhn unit.  $R_g$  was measured for two PECs of different chain length, and as a function of temperature. D-PMAPTAI (see Figure S3 and Table S1) was used to make a deuterium labelled PEC by mixing 25 mol% P(D-MAPTAI) with 75 mol% PMAPTAC, and PAMPS in stoichiometric ratios to obtain complexes with polymer chain lengths given in Table 4. Dilution of the deuterated chains in this way simplifies the analysis by separating interchain from intrachain correlations.<sup>47</sup> To ensure that the deuterated polymers were the only segments contributing to coherent scattering, the non-deuterated components were contrast matched with a 1:4 mixture of  $D_2O$  and  $H_2O$ . Figure 1 shows the neutron scattering profile from the two PEC samples (see also Figure S4) soaked in a 0.1 M NaSCN 1:4  $D_2O$ :H<sub>2</sub>O solution.

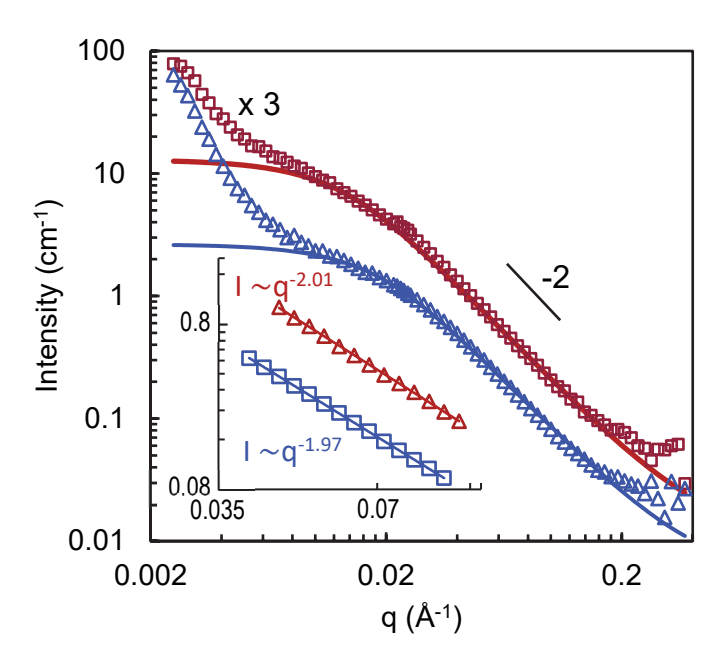


**Figure 1.** Small angle neutron scattering of PEC **d-A** (upper curve,  $n_{DMAPTA} = 1363$ , Table 4) displaced for clarity by a factor of 3 and PEC **d-B** (lower curve  $n_{DMAPTA} = 609$ , Table 4), both in 0.10 M NaSCN at 25 °C. 25% of the PMAPTA was pure D-MAPTA homopolymer. The

nondeuterated components were contrast matched with a mixture of 1:4  $D_2O/H_2O$ . The fits (solid lines) are to Gaussian coils with respective  $R_G$  of 11.3 and 8.0 nm. Inset shows the Guinier region: intensity from 0.08 to 0.8 and q from 0.04 to 0.09 Å<sup>-1</sup>

In intermediate q ranges (0.02 Å<sup>-1</sup> < q < 0.2 Å<sup>-1</sup>), the scattering is predominantly from length scales of the polymer coil size (D-PMAPTA in this case). SASview was used to fit the form factor, P(q) for Gaussian chains:

$$P(q) = \frac{2(e^{-x} + x - 1)}{x^2}$$
 [2]

where  $x = q^2R_g^2$ . The scattering intensity I(q) decays with q as  $I(q) \sim q^{-2}$  (Figure 1 inset and Figure S4) which is a feature of scattering from Gaussian chains. The  $R_g$  measured for PECs **d-A** and **d-B** was 11.3 and 8.0 nm, respectively. The Kuhn length, b, was calculated from the polymer contour length nl (n is the number of monomer repeat units and l = 0.252 nm is the length between repeat units along the backbone) such that  $b = 6R_g^2/nl$ . b was determined to be 2.23 and 2.50 nm for the longer and shorter chains in Figure 1, respectively, for an average of 2.37  $\pm$  0.19 nm. The Kuhn length for PAMPS in a  $\theta$ -solvent was reported to be 2.4 nm.<sup>48</sup> The number of monomer units,  $n_K$ , in a Kuhn length is b/l = 9.4. Scattering from PEC **d-B** ( $n_{DMAPTA} = 609$ ) over the same qrange was measured as the system was heated (5 to 65 °C, Figure S4) and the fitted  $R_g$  was found to be constant within error (8.0  $\pm$  0.20 nm) as a function of temperature.

**Critical Salt Concentration, CSC**. Sufficiently concentrated salt solutions swell, then dissolve, most PECs, effectively reversing the liquid-liquid phase separation that caused them.<sup>49</sup> The point at which this occurs, often judged by eye, or measured with turbidimetry, is the CSC (also termed "salt resistance"<sup>50</sup>). The CSC, a readily accessible point on the phase diagram of PECs in equilibrium with the dilute phase, depends on molecular weight: the CSC for shorter chains is lower.<sup>23</sup> The CSC also depends strongly on the chemical nature of MA: salts containing ions at the hydrophobic end of the Hofmeister series are more effective at dissolving PECs. Some PECs which do not show an apparent CSC at any [MA]<sub>s</sub> for a particular salt may be dissolved with a

more hydrophobic salt.<sup>41</sup> The CSCs for three PMAPTA/PAMPS pairs in NaSCN are shown in Figure 2.

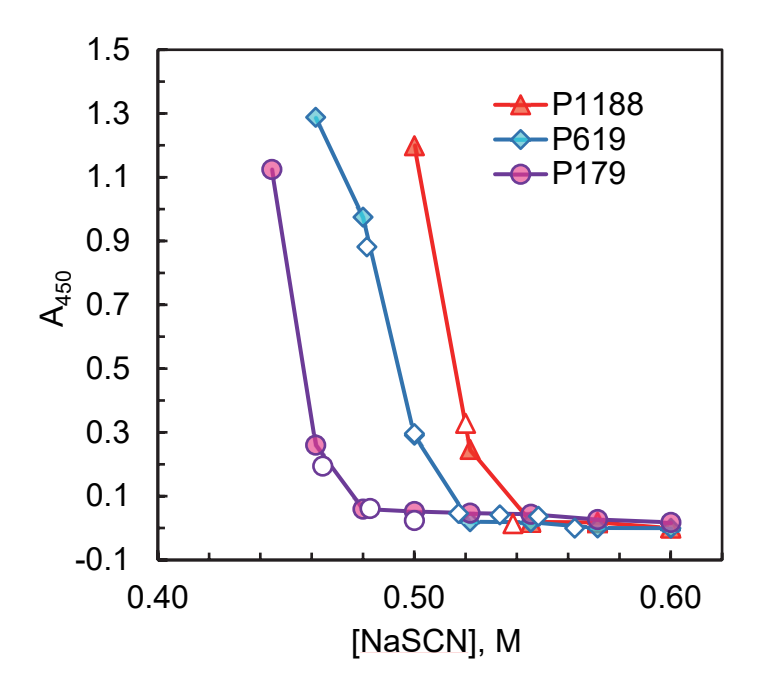


**Figure 2.** Measurement of the critical salt concentration of 1 mg mL<sup>-1</sup> PMAPTA/PAMPS using PECs P179 (circles); P619 (diamonds); and P1188 (triangles) pairs, all with low polydispersity (see Tables 1 and 3). Turbidity is given by the absorbance at a wavelength of 450 nm (A<sub>450</sub>) at room temperature. The CSC is taken to be [NaSCN] where A<sub>450</sub> drops to zero. First, 0.6 M NaSCN was added to 3 mg PEC, which was slightly above [NaSCN]<sub>S,CSC</sub> (absorbance  $\approx$  0). Water was then added to dilute the NaSCN and bring the solution below the [NaSCN]<sub>S,CSC</sub> in the "desalting" or "reverse" method (filled symbols). Then, NaSCN was added to the precipitated PEC to dissolve it again (the "forwards" method, open symbols).

**Specific Doping of PEC by NaSCN.** Below the CSC, MA added to solution is assumed to "dope" the PEC, represented by Equation 3, in a site-specific model. (In contrast, MA "shields" the polymer charges in continuum electrostatics models)

$$[Pol^{+}Pol^{-}]_{PEC} + yM_{s}^{+} + yA_{s}^{-} \rightarrow [(Pol^{+}Pol^{-})_{1-y} + (Pol^{+}A^{-}Pol^{-}M^{+})_{y}]_{PEC}$$
[3]

where *y* is the fraction of intrinsic sites converted to extrinsic ones, "s" is the solution phase and "PEC" is the PEC phase. Equation 3 assumes all salt in the PEC breaks Pol<sup>+</sup>Pol<sup>-</sup> pairs, as in Scheme 1. However, it has been found experimentally<sup>23, 51</sup> and computationally<sup>24</sup> that MA does not necessarily break Pol<sup>+</sup>Pol<sup>-</sup> pairs and, especially near the CSC,<sup>34</sup> much of the salt exists as coions rather than the counterions implied by Equation 3. A more accurate representation of the disposition of ions within a PEC is

$$[Pol^{+}Pol^{-}]_{PEC} + rM_{s}^{+} + rA_{s}^{-} \rightarrow [(Pol^{+}Pol^{-})_{1-fr} + (Pol^{+}A^{-}Pol^{-}M^{+})_{fr} + (M^{+}A^{-})_{(1-f)r}]_{PEC}$$
 [4]
Intrinsic Extrinsic co-ions

where r is the molar ratio of total MA in the PEC to Pol<sup>+</sup>Pol<sup>-</sup> and f is the fraction of MA within the PEC acting as counterions. Thus, y = fr. Figure 3 shows r as a function of [NaSCN]<sub>s</sub>. The data is also presented as [NaSCN]<sub>PEC</sub> versus [NaSCN]<sub>s</sub>, which makes it clear that the concentration of MA in the PEC is more than that in the supernatant at equilibrium, in conflict with most electrostatics-based theory. <sup>10</sup> As with most PEC doping responses, <sup>23,51</sup> there is a small intercept on the [MA]<sub>s</sub> axis, giving a negative intercept on the r axis (here, about -0.02), probably due to a combination of the residual ions from excess PMAPTA<sup>+</sup> (about 2%) and the osmotic pressure of the chains themselves. These nonidealities are hard to avoid, <sup>27</sup> as all undoped PECs contain a few extrinsic sites (see Table 3), making it difficult to approach truly ion-free PEC.

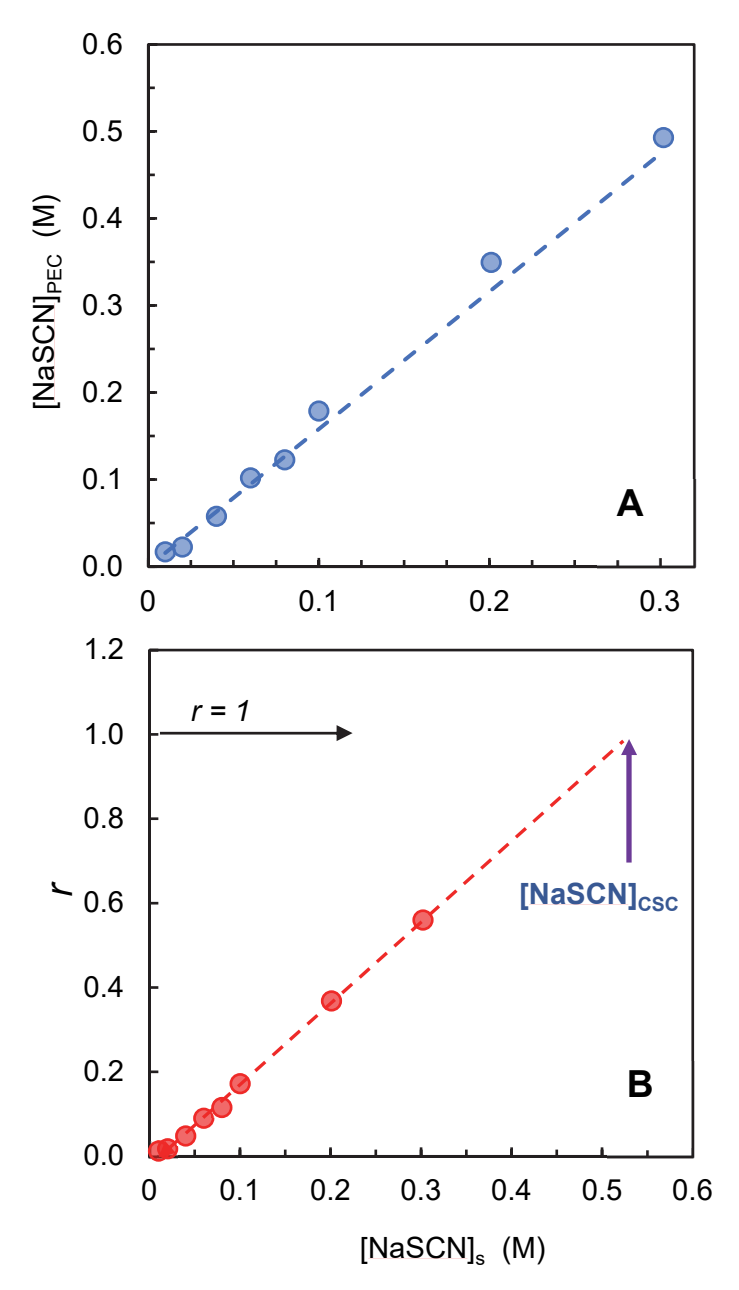


**Figure 3.** Doping of PMAPTA/PAMPS PEC with NaSCN at room temperature. **A:** molar concentration of NaSCN in the PEC, [NaSCN]<sub>PEC</sub>, as a function of [NaSCN] in the solution or "dilute phase," [NaSCN]<sub>s</sub>. The dashed line is provided by Equation 10, where f was assumed to be = 1 and  $\Delta$ H<sub>PEC</sub> was measured to be +2255 J mol<sup>-1</sup>; [NaSCN]<sub>PEC</sub> = 1.58[NaSCN]<sub>s</sub>. **B:** ratio r = [NaSCN]<sub>PEC</sub>/[PE]<sub>PEC</sub> versus [NaSCN]<sub>s</sub>. The dotted line gives r = 1.93[NaSCN]<sub>s</sub> – 0.02. From this fit, at r = 1, [NaSCN]<sub>s</sub> = 0.53 M which is close to the experimental CSC (Figure 2).

**Ion Dynamics as a Reporter of Polymer Repeat Unit Dynamics**. Ion transport in PECs can be modeled by hopping between adjacent segments of the same charge.<sup>40</sup> e.g.

$$Pol_1^+ Pol_1^- + Pol_2^- Na^+ \to Pol_1^- Na^+ + Pol_1^+ Pol_2^-$$
 [5]

Because counterion dynamics are coupled to, and limited by, polymer dynamics,  $^{52}$  the ion hopping rate  $\omega_{\text{ion}}$  is assumed to be the same as the Pol+Pol- breaking rate.  $^{40}$  The diffusion coefficient of NaSCN was determined by monitoring the conductivity of a solution of fresh water which was poured on top of a doped PEC film. The fraction of the released salt ( $\psi = M_{NaSCN_t}/M_{NaSCN_{t=\infty}}$ ), where  $M_{NaSCN_t}$  is the amount of NaSCN released at time t, was used to evaluate the salt diffusion coefficient,  $D_{\text{ions}}$  of NaSCN (cm<sup>2</sup> s<sup>-1</sup>) using the equation for diffusion out of/into a plate:  $^{53}$ 

$$\psi = \frac{M_t}{M_{\infty}} = 1 - \sum_{n=0}^{\infty} \frac{8}{(2n+1)^2 \pi^2} exp \left[ \frac{-D_{ions}(2n+1)^2 \pi^2 t}{4\sigma^2} \right] = \left( \frac{2\sqrt{D_{ions}t}}{\sigma\sqrt{\pi}} \right)_{\psi < 0.6}$$
 [6]

where  $\sigma$  is the thickness of the PEC. The boundary conditions for Eq. 6 are: diffusion from one side of a parallel plate, assume uniform distribution of ions in the PEC at t = 0 and the concentration of ions at the surface and in the bulk water  $\rightarrow$  0, ensured by a large volume of water and brisk stirring at the interface. The slope of the line in Figure 4A is the linear limit of Equation 6, valid for  $\psi$  < 0.6. Average ion hopping frequencies can then be calculated by assuming three-dimensional hopping between nearest next neighbors:

$$\omega_{ion} = \frac{6D_{ions}}{d^2}$$
 [7]

Where d is the hopping distance or the distance between Pol<sup>+</sup>Pol<sup>-</sup> pairs (Table S2). The relaxation rate slows with cooling according to the Arrhenius equation with activation energy  $E_i$  (J mol<sup>-1</sup>):

$$\omega_{ion} = A_1 e^{-E_i/RT}$$
 [8]

 $E_i$  was calculated from the slope of InD vs. 1/T to be 18.2 kJ mol<sup>-1</sup> and  $A_1$  was found from the intercept of Figure 4B:  $1.36 \times 10^{12} \text{ s}^{-1}$ .

0.6

0.4

0.2

0.2

0.5.5 °C

0.25.2 °C

44.7 °C

54.6 °C

64.8 °C

0.0

0 10 20 30 40

t<sup>0.5</sup> (s<sup>0.5</sup>)

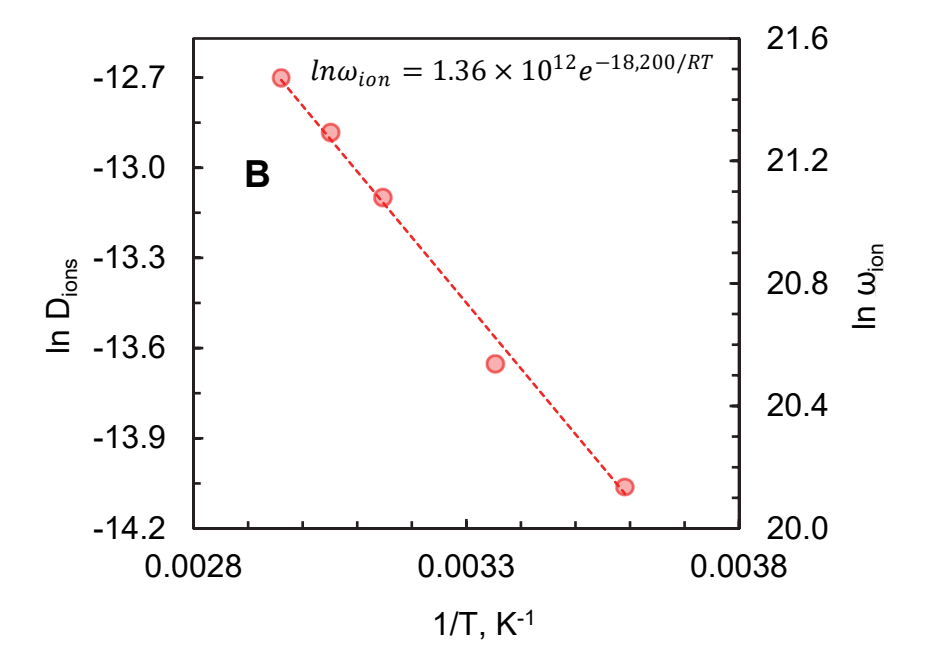


**Figure 4. A**. Fraction  $\psi$  of NaSCN released into water as a function of  $t^{0.5}$  (s<sup>0.5</sup>) at various temperatures from a PMAPTA/PAMPS PEC doped in 0.1 M NaSCN. Solid lines are the fit to Equation 6 using the fitted diffusion coefficients (cm<sup>2</sup> s<sup>-1</sup>) in **B** (left axis). The hopping frequencies

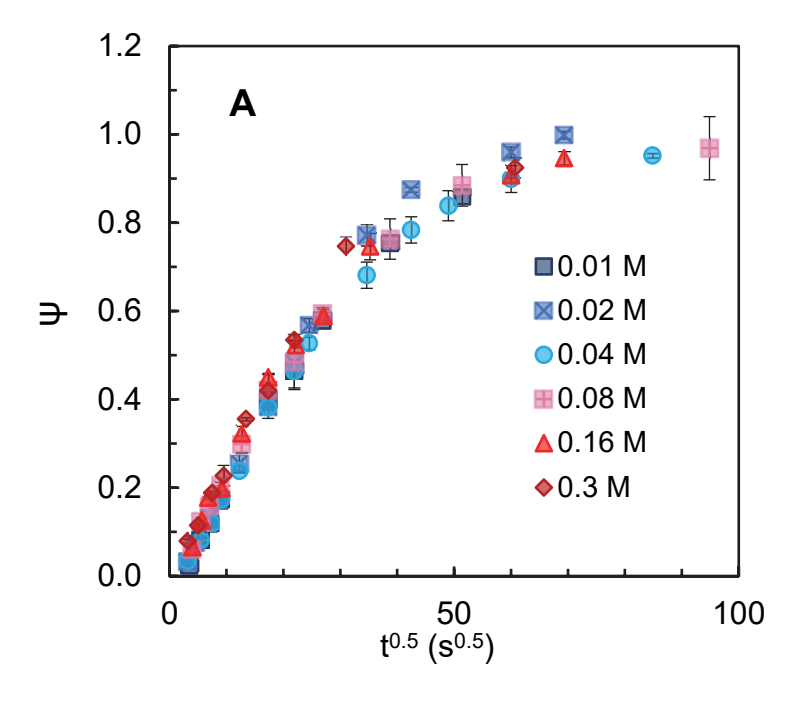
were calculated using  $\omega_{ion} = \frac{6D_{ions}}{d^2}$  and an average distance *d* between Pol<sup>+</sup>Pol<sup>-</sup> pairs of 0.95 x 10<sup>-7</sup> cm (in 0.1 M NaSCN, Table S2). The slope gives an activation energy of 18.2 kJ mol<sup>-1</sup> and an intercept D<sub>0</sub> of 2.05 x 10<sup>-3</sup> cm<sup>2</sup> s<sup>-1</sup> and A<sub>1</sub> = 1.36 x 10<sup>12</sup> s<sup>-1</sup>.

The tracer diffusion coefficient of SCN $^{-}$ ,  $D_{SCN}$ , at different [NaSCN] $_{s}$  was determined by measuring the fraction of radioactive thiocyanate,  $S^{14}CN^{-}$ , released into a solution of non-radioactive NaSCN of the same concentration (Figure 5).  $D_{SCN}$  remained surprisingly similar (Figure 5B) over the range of [NaSCN] $_{s}$ , another indication that SCN $^{-}$  clings to MAPTA $^{+}$  as it hops through the PEC. In fact, the only reason for the variation of  $D_{SCN}$  is from the slight increase in film thickness  $\sigma$  as the PEC is doped. There is little evidence that NaSCN accelerates dynamics by "screening" Pol $^{+}$ Pol $^{-}$  electrostatic interactions. $^{17}$ 

 $D_{ions}$  represents the coupled diffusion coefficient between Na<sup>+</sup> and SCN<sup>-</sup>, while  $D_{SCN}$  is the tracer or single ion coefficient for SCN<sup>-</sup>. The two are related by<sup>54</sup>

$$D_{ions} = \frac{2D_{Na}D_{SCN}}{D_{Na} + D_{SCN}}$$
 [9]

where  $D_{Na}$  is the tracer diffusion coefficient for  $Na^+$ . Because the coefficient at 25 °C for  $D_{ions}$  and  $D_{SCN}$  are similar (1.3 x 10<sup>-6</sup> and 1.0 x 10<sup>-6</sup> cm<sup>2</sup> s<sup>-1</sup>, respectively),  $D_{Na}$  must be close to  $D_{SCN}$ .



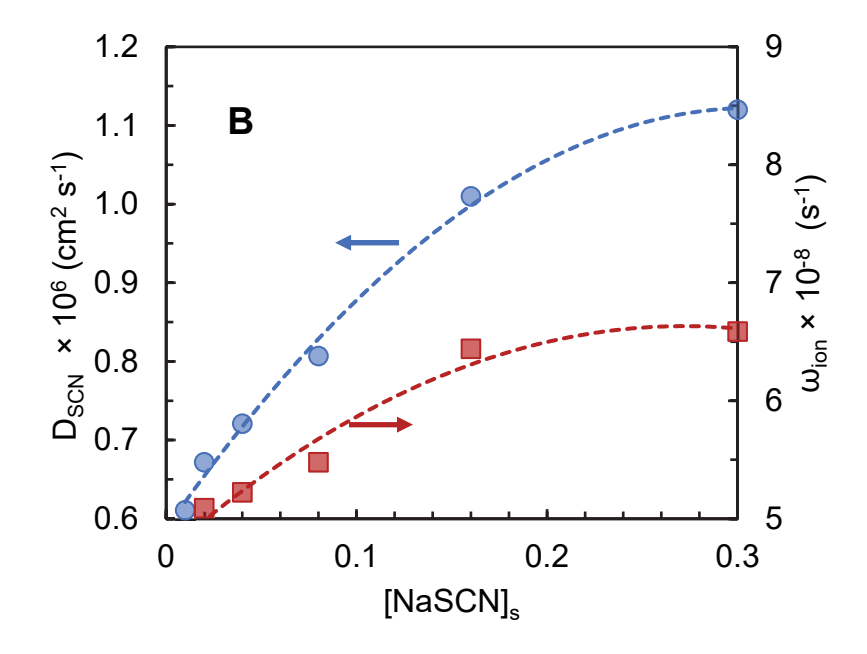


**Figure 5. A**; Fraction of radiolabeled  $S^{14}CN$ ,  $\psi$ , exchanged with 10 mL unlabeled NaSCN as a function of time  $^{0.5}$  (s  $^{0.5}$ ) at [NaSCN]<sub>s</sub> = 0.01, 0.02, 0.04, 0.08, 0.16 and 0.3 M. Room temperature. **B**; The diffusion coefficient fits to Equation 6 for  $\psi$  < 0.6 as a function of [NaSCN]<sub>s</sub> (blue circles). lon hopping frequencies were calculated from Equation 7 using *d* values given in Table S2 (red squares). The dotted lines are guides to the eye.

**Linear Viscoelastic Response (LVR).** Rheology was used the monitor the LVR of PEC pairs of various lengths. The storage and loss modulus were measured at a strain of 0.1% and at different temperatures in the frequency range  $0.01 < \omega < 100$  rad s<sup>-1</sup>. Time-temperature superposition, TTS, was used to study the dynamics across a wider range of frequencies in Figure 6. Individual TTS plots of the pairs along with shift factors  $a_T$  and  $b_T$  are given in Figure S5.

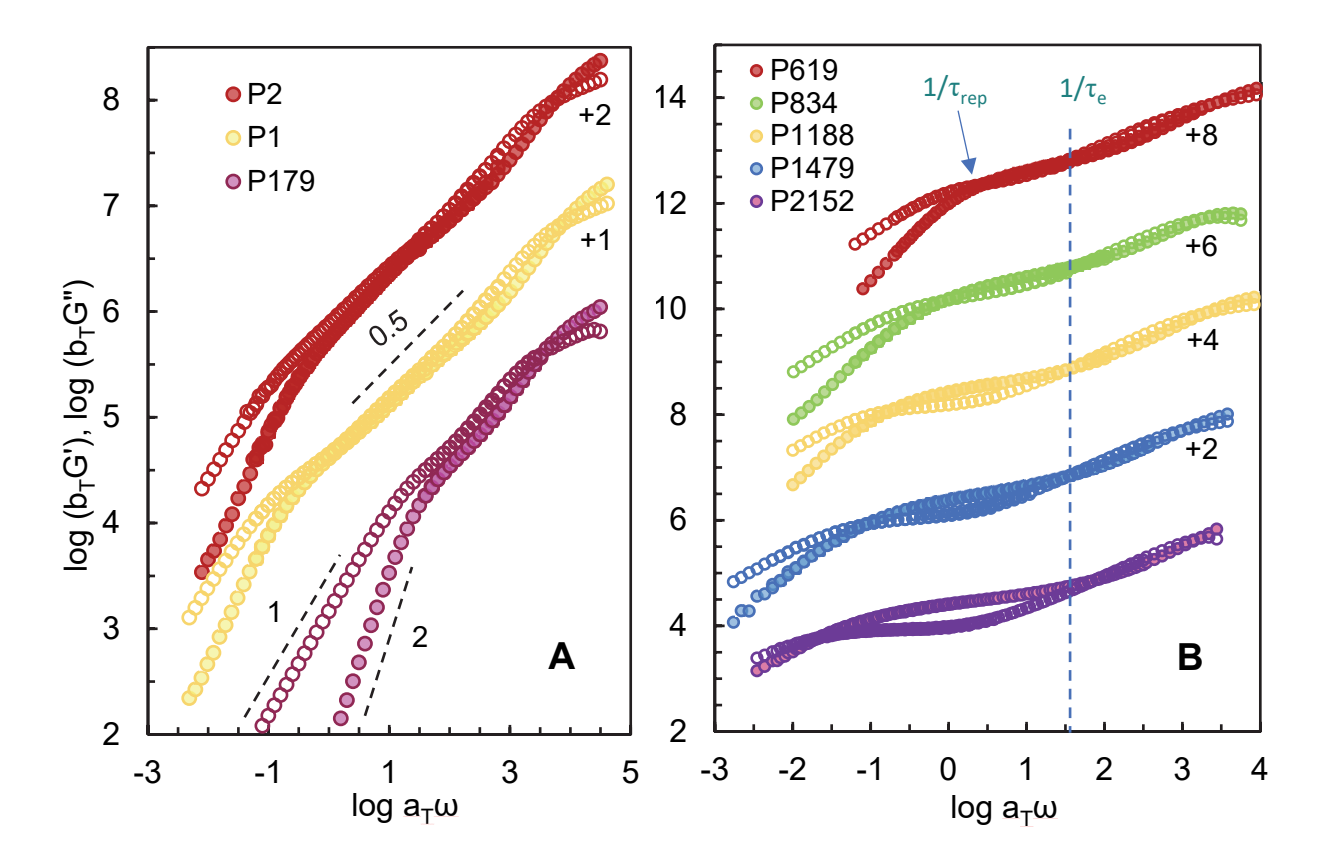


**Figure 6**. Linear viscoelastic response of PMAPTA/PAMPS PECs in 0.01 M NaSCN. Storage and loss modulus, G' and G" (Pa), as a function of frequency (in rad s<sup>-1</sup>). Shift factors a<sub>T</sub> and b<sub>T</sub> for time-temperature superposition are given in Supporting Information Figure S5. Reference temperature is 25 °C. **A,** PEC below entanglement and mismatched pairs. **B**, pairs with matched molecular weights, all above the entanglement molecular weight.

**Table 5**. The dynamic crossover lifetimes  $\tau_{rep}$ ,  $\tau_e$  and  $\tau_0$  (s), storage modulus at the rubbery plateau  $G_o$  (Pa), number of Kuhn segments between entanglements  $N_e$ , and zero shear viscosity  $\eta_o$  (Pa s) of the PMAPTA/PAMPS pairs at  $T_{ref} = 25$  °C and [NaSCN]<sub>s</sub> = 0.01 M.

$\mathbf{P}_{nav}$	$ au_{rep}$ (s)	$ au_{ m e}\left({ m s} ight)$	$ au_0$ (s)	G <sub>o</sub> (Pa)	$N_{e}$	η₀ (Pa.s)	$G_{o}\tau_{rep}$
P179	-	-	2.5 x 10 <sup>-4</sup>	-	-	2.58 x 10 <sup>3</sup>	-
P619	0.35	0.029	3.6 x 10 <sup>-4</sup>	38000	14	2.35 x 10 <sup>4</sup>	1.33 x 10 <sup>4</sup>
P834	1.26	0.020	5.6 x 10 <sup>-4</sup>	32400	16	5.39 x 10 <sup>4</sup>	4.08 x 10 <sup>4</sup>
P1188	5.8	0.028	4.8 x 10 <sup>-4</sup>	33100	16	1.91 x 10 <sup>5</sup>	1.89 x 10 <sup>5</sup>
P1479	11.3	0.025	3.5 x 10 <sup>-4</sup>	28200	19	2.88 x 10 <sup>5</sup>	3.19 x 10 <sup>5</sup>
P2152	45.6	0.012	5.8 x 10 <sup>-4</sup>	26900	20	1.14 x 10 <sup>6</sup>	1.23 x 10 <sup>6</sup>
P1	-	-	4.8 x 10 <sup>-4</sup>	-	-	2.71 x 10 <sup>3</sup>	-
P2	-	-	5.2 x 10 <sup>-4</sup>	-		2.89 x 10 <sup>3</sup>	-

Fig. 6B gives G' and G" for pairs P619, P834, 1188, P1479, P2152, all above entanglement as indicated by the two dynamic crossover points at lower frequencies:  $\omega_{rep}$  and  $\omega_{e}$ .  $\tau_{rep}$  =  $1/\omega_{rep}$  describes the relaxation time of the longest dynamic length scale corresponding to a polymer chain reptating out of a tube.

Table 5 summarizes the characteristic LVR parameters for PEC pairs. Characteristic relaxation times are read directly from the G' and G" crossing points in Figure 6: reptation time,  $\tau_{\rm rep}$ ; Rouse relaxation time of a chain length between entanglements,  $\tau_{\rm e}$ ; relaxation time of a Kuhn (ideal) monomer,  $\tau_{\rm 0}$ . Plateau modulus G<sub>0</sub> was taken as G' at the maximum of G'/G" (minimum of  $\tan\delta$ ). The number of Kuhn monomers between entanglements,  $N_{\rm e}$  =  $M_{\rm e}/M_0 n_{\rm K}$ , where  $M_{\rm e}$  was calculated from Equation 11.

## DISCUSSION

In order to understand the response of PECs to variables such as temperature, molecular weight and salt concentration, many parameters must be known, including the coil size, and the dependence of coil size on temperature. This work attempts to measure these on the same, well-behaved system to enable theoretical and quantitative descriptions. Because charged monomers were used for synthesis, the resulting polyelectrolytes were fully charged. PMAPTAC and PAMPS yield a liquid-like PEC well above T<sub>g</sub> at room temperature, similar to conditions used for many neutral polymers to probe dynamics in the melt phase. The quaternary ammonium and sulfonate charged groups on the respective polyelectrolytes are strongly charged i.e. remain fully ionized over a wide range of solution pH. Due to their enhanced stability against hydrolysis, <sup>55</sup> acrylamido monomers were preferred over acrylates. The acrylamido group also places hydrophilicity near

the backbone, as opposed to phenyl pendant groups such as those in poly(styrene sulfonate), a widely used polyelectrolyte.

Narrow molecular weight distributions of PMAPTAC and PAMPS were prepared using classical fractionation techniques (see Table 1 and Figure S1 for details on polyelectrolyte length and distribution). The polymer chains did not have hydrophobic end units, believed to have caused anomalous results in prior PEC SANS characterization.<sup>56</sup> Solution NMR was used to verify that PECs were close to stoichiometric (see Table 3 for Pol<sup>+</sup>Pol<sup>-</sup> ratios and Figure S2 for NMR spectra and peak assignments). Non-stoichiometric PECs tend to be softer than stoichiometric ones because the charge pairing density is lower and the water content is higher.<sup>57</sup> In the present case, the level of nonstoichiometry was less than 3%, which was considered acceptable for the current set of experiments. One well-entangled polyelectrolyte pair, P1479, was selected for more intensive studies on the effect of salt content on properties. Using sensitive radiolabeling techniques, the stoichiometry for P1479 was determined to be 1.018 Pol<sup>+</sup>:Pol<sup>-</sup> (i.e. 1.8% off-stoichiometric; Table 2).

Coil Dimensions. Few studies have been reported on SANS of synthetic PECs. The first found that chains were close to Gaussian,<sup>58</sup> a conclusion also reached by Spruijt et al.,<sup>56</sup> who used PECs made from weak polyelectrolytes poly(acrylic acid), PAA, and poly(N,N-dimethylaminoethyl methacrylate). However, the estimated Kuhn length in that work varied strongly from 3.5 to 16 nm. A long Kuhn length would support the "twisted pair" model of Hamad et al., 27 but a review by Larson et al. 29 presents a variety of shorter Kuhn lengths for charged polymers and concludes the Kuhn high lengths of Spruijt et al. may be upper limits. Compact Gaussian coils are expected if there are no long-range perturbations, such as electrostatic repulsions and extensive solvation. All well-paired PECs are locally neutral and the amount of water admitted to the PEC is low relative to dilute solution. Fares et al. found Rq to be independent of salt concentration,59 in contrast to the typical response of individual polyelectrolytes, possibly a consequence of the high Pol<sup>+</sup>Pol<sup>-</sup> charge density (>1 M) within PECs. SANS studies of PECs report a "low q upturn," attributable to density fluctuations approaching the 1 µm length scale, although the materials remain transparent to the eye. 56, 58, 60-61 This long-range feature, probably not a result of thermal fluctuations, as it changes little with temperature (Figure S4), may be due to weak microphase separation between deuterated and non-deuterated polymers. The negligible temperature dependence of coil size in Figure S4 is similar to that found in neutral polymers under θ-conditions. For example, Zirkel et al. found that the  $R_g$  of poly(ethylethylene) in a  $\theta$ -solvent changed by less than 2% over the same temperature range as that used here. 62

**PEC Stability.** The CSC in NaSCN of three pairs of PMAPTA/PAMPS was measured using turbidimetry. The thiocyanate ion is at the hydrophobic end of the Hofmeister series, making it particularly effective at breaking Pol<sup>+</sup>Pol<sup>-</sup> pairs.<sup>63</sup> Low polydispersity P179, P619, and P1188 yielded steep room temperature CSCs at around 0.55 M NaSCN (Figure 2). Figure 2 reveals only a mild dependence of CSC on molecular weight, as expected for longer polymers. Approaching the CSC from low to high [NaSCN]<sub>s</sub> (the more conventional "forwards" method) gives the same result as from the reverse method (also known as "desalting" <sup>2,64</sup>). This is strong evidence that the composition of this (liquid-like) PEC is in equilibrium with the solution composition. Being kinetically sluggish, more solid-like PECs are expected to show distinct metastable phases.<sup>65</sup>

The CSC of wide MWD PMAPTA/PAMPS was found to be less sharp (Figure S6) and the forwards salt addition did not track the desalting curve. Because the effective association constant between associated polyelectrolytes in PEC and individual polymers in solution is extremely high,  $^{66}$  over most [MA]<sub>s</sub> < [MA]<sub>CSC</sub> negligible amounts of polyelectrolyte are expected in the dilute phase, either as individual molecules or "quasisoluble" clusters. Quasisoluble PEC nanoparticles are favored when there is nonstoichiometry and a length mismatch, which means for a wide  $\Theta$  sample, the forwards addition may not generate the same particle size distributions as the reverse, generating hysteresis in the absorbance and giving the appearance of metastability.

**PEC Ions: Counter- or Co-?** To date, there are no experimental methods that directly indicate whether an ion in a PEC is a counterion or a co-ion. Without this knowledge, the density of Pol<sup>+</sup>Pol-pairs as a function of [salt] remains unknown. Presumed fast exchange between the two ion environments complicates such a measurement. If the fraction f were approximately = 1, y = r. There are two systems where f is believed to approach 1: glassy PECs have limited free volume, forcing Pol<sup>+</sup>Pol<sup>-</sup> to break at low doping.<sup>23</sup> Alternatively, ions with specific affinity for either Pol<sup>+</sup> or Pol<sup>-</sup> would bias the MA<sub>PEC</sub> population in favor of counterions. Thiocyanate is, potentially, such an ion. Affinity (specificity) for Pol<sup>+</sup> or Pol<sup>-</sup> is revealed by an *endothermic* heat of complexation: polymer pairing causes the *loss* of a specifically "bound" ion.<sup>51</sup>

Isothermal calorimetry (ITC, detailed procedure described in Supporting Information) was carried out to measure the heat of complexation,  $\Delta H_{PEC}$ , between PMAPTA(SCN) and PAMPS(Na). The ITC thermogram (Figure S7) showed net endothermic complexation with  $\Delta H_{PEC}$  = +2255 J mol<sup>-1</sup>, indicating significant attractive MA specificity, probably SCN<sup>-</sup> for MAPTA<sup>+</sup>. The distribution of MA between PEC and supernatant is the result of a Donnan equilibrium, described by<sup>51</sup>

$$\frac{[MA]_{PEC}}{[MA]_{S}} = e^{f\Delta H_{PEC}/2RT}$$
 [10]

The  $e^{f\Delta H_{PEC}}$  term represents the departure from an ideal Donnan equilibrium driven by entropy alone. If f = 1, Eq. 10 for the current PEC system would yield [NaSCN]<sub>PEC</sub> = 1.58[NaSCN]<sub>s</sub>, which is shown as the dotted line, predicting the experimental [NaSCN]<sub>PEC</sub> results in Figure 3 well.

A second piece of information supporting the assumption that f = 1 over much of the [NaSCN]<sub>PEC</sub> is obtained by extrapolating r versus [NaSCN]<sub>s</sub> to r = 1. At this point, the number of salt ions equals the number of polyelectrolyte charges and, if f = 1, y = r and the PEC should be dissociated. Indeed, at r = 1, the [NaSCN]<sub>s</sub> is at the CSC (Figure 3B).

As a final and direct indication of the disposition of ions within the PEC, FTIR was performed on various SCN⁻- containing systems. The wavelength of the C≡N stretch in SCN⁻ (and in other cyano systems) is known to depend on the solvation environment.<sup>71</sup> This "vibrational solvatochromism" can be related to a change in the local electric field, or Stark effect, once all the contributions to this field are accounted for. SCN groups are also used as site-specific vibrational probes of protein electrostatics.<sup>72</sup> Figure 7 shows a clear, albeit small, 4.6 cm⁻¹ shift for SCN⁻ associated with PMAPTA⁺ in a counterion environment (PMAPTA(SCN) solution). The identical shift is seen for SCN⁻ in PEC (in 0.3 M NaSCN for a doping level of about 0.6), whereas in a solution of NaSCN or NaSCN with PAMPS, v<sub>SCN⁻</sub> is at 2064 cm⁻¹, reflecting an unassociated or co-ion environment. This is the first reported direct measurement of the ion environment within a

PEC. 2060 cm<sup>-1</sup> corresponds to a 6.2 x  $10^{13}$  Hz = 2.6 x  $10^{-15}$  s relaxation time, much shorter than the residence time of SCN<sup>-</sup> on MAPTA<sup>+</sup> (about 2 ns at room temp, see below). It is assumed that SCN<sup>-</sup> in a PEC co-ion environment would be reflected by intensity at 2064 cm<sup>-1</sup>. All these pieces of evidence support the assumption that f = 1, at least up to 60% doping, and that each NaSCN breaks a charge pair crosslink as in Scheme 1. The precise nature of the MAPTA<sup>+</sup>:SCN<sup>-</sup> association, whether a contact ion pair or a solvent separated pair, is not known. Though SCN<sup>-</sup> is more likely to be specifically located next to MAPTA<sup>+</sup> than Na<sup>+</sup> is next to AMPS<sup>-</sup>, one SCN<sup>-</sup> still breaks one Pol<sup>+</sup>Pol<sup>-</sup> pair.

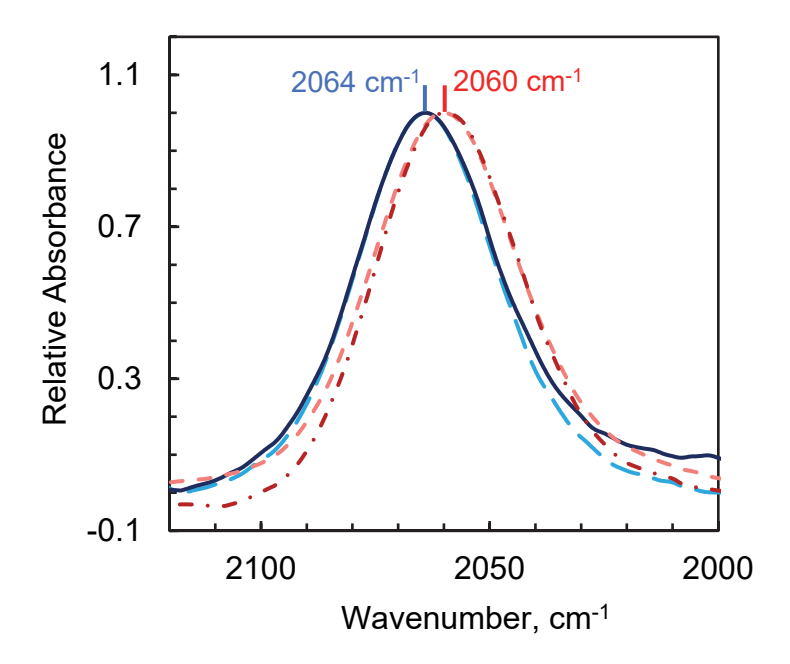


**Figure 7.** Normalized ATR-FTIR spectra of CN stretch in: 1.0 M NaSCN, blue long dash; 0.6 M NaSCN in 1.0 M PAMPS-Na, solid blue line; 1.0 M PAMPTA(SCN), red short-dashed line; and PMAPTA/PAMPS PEC doped in 0.3 M NaSCN, red dash-dot. Spectral resolution, 0.5 cm<sup>-1</sup>. Room temperature. When SCN<sup>-</sup> is associated with PMAPTA, either in solution or in the PEC, there is a ~4.6 cm<sup>-1</sup> red shift in the C≡N absorption band.

Without a direct measure of f, and if f varies as a function of [salt], it becomes difficult to relate the density of Pol+Pol- pairs to external salt concentration. As long as f is > 0, Pol+Pol- pairs will be broken on doping and the viscoelasticity will change to lower values of modulii and viscosity. Ghasemi et al.<sup>24</sup> have computed the value of f as a function of [salt]. If there are measurable enthalpy changes on complexation, the magnitude of f may be extracted by determining the ratio [MA]<sub>PEC</sub>/[MA]<sub>s</sub> and using Equation 10. In certain cases, f decreases with doping, e.g. when  $\Delta H_{PEC}$  is exothermic, and the product fr never reaches 1. In such a scenario, a CSC is not observed.<sup>41</sup>

The Nature of the "Sticker". Physical interactions between polymers are often called "stickers." Charge pairing interactions break and reform at a fast rate, about 5 x 108 s<sup>-1</sup> at room temperature according to Figure 5. Such a short sticker lifetime is on the order of the fastest relaxation time in neutral polymers³ and would not be effective by itself at slowing chain dynamics. In fact, in undoped PECs, there are no "available" extrinsic sites, so neighboring two pairs, or a quad of charges, must exchange places simultaneously if they are to move. Pair exchange has twice the activation energy as pair breaking and occurs much more slowly. In effect, almost all of the pair breaking events lead to recombination of the same pair and only in the rare event that two pairs break simultaneously, lifetime  $\tau_q$ , can chains move relative to each other. This is an example of a "renormalized" sticker lifetime,  $\tau_b^*$ . In the present system,  $\tau_q = \tau_b^* = 7.3 \times 10^{-13} \exp{(\frac{36,900}{RT})}$  (see Supporting Information Figure S8 for more details). To compare with the LVR data (Figure 6, Table 5)  $\tau_q$  must be further normalized so that  $\tau_0$  represents a Kuhn length of stickers, which is 9.4 pairs. The estimated  $\tau_0$  (see Supporting Information) is about 2 x 10<sup>-4</sup> s, which is fairly close to the value read from the  $\tau_0$  crossover.

**Sticky Reptation.** From Figure 6 and Table 5, the measured  $G_0$ ,  $\tau_e$ , and  $\tau_0$  do not depend significantly on chain length, as expected, whereas  $\tau_{rep}$  becomes significantly slower with longer chains. The terminal region shows the expected  $\omega^1$  and  $\omega^2$  scaling for G'' and G', respectively. The ratio of  $\tau_{rep}/\tau_e$  vs.  $n_{avg}$  was used to determine  $n_c$ , the critical number of monomer units for entanglement (Figure S9).  $n_c$  = 347 ( $N_c$  = 37) was found to be 2 - 3 times the value of  $n_e$ , which is similar to neutral polymers.

Below  $n_c$ , only the "monomer time"  $\tau_0$  was observed (Figure 6A), at values similar to those for entangled pairs. The similarity of  $\tau_0$  and viscosity for the mismatched pairs P1 and P2 support the assumption that the chain dimensions (i.e. Kuhn lengths) for PMAPTA and PAMPS are similar. In P1 and P2 the shorter chain is below  $n_c$  and  $G' \approx G'' \sim \omega^{0.5}$ . Over much of the frequency range, which are the gel criteria according to Winter and Chambon. For these PECs, the smaller polyelectrolyte chains act as crosslinks between the longer chains of opposite charge.

The expression for the plateau modulus  $G_0$  depends on polymer volume fraction  $\phi$  (for 0.01 M NaSCN  $\phi$  = 0.45), and density,  $\rho$ , and has the form<sup>74</sup>

$$G_0 = \frac{4\rho RT\emptyset}{5M_e}$$
 [11]

where  $M_e$  is the molar mass between entanglements.  $G_0$  is assumed to be unaffected by sticker units.<sup>37</sup> The number of monomer units between entanglements,  $n_e$ , is  $M_e/M_0$ , where  $M_0$  is the molar mass of a repeat unit, here an average between MAPTA and AMPS of 196 g mol<sup>-1</sup>. Sticky reptation dynamics for entangled polymers have been treated theoretically by Rubinstein and Seminov<sup>37</sup> and others.<sup>38</sup> The sticky reptation time  $\tau_{rep}$  (also called the "disengagement time") is<sup>37</sup>

$$\tau_{rep} \approx \tau_b^* (f_s p_{inter})^2 N / N_e$$
 [12]

Where  $f_s$  is the number of stickers per chain,  $\tau_b^*$  is the renormalized sticker lifetime and  $p_{inter}$  is the fraction of intermolecular (as opposed to intramolecular) stickers. In PECs, because all polymer repeat units are forced to pair with other units,  $p_{inter} = 1$ . In the LVR data presented in Figure 6 and Table 5 the relaxation time  $\tau_0$  corresponds to a Kuhn length and F corresponds to the number of Kuhn length stickers per chain,  $F = f_s/n_K$ , thus

$$\tau_{ren} \approx \tau_0(F)^2 N / N_e \tag{13}$$

For undoped PEC, F = N and

$$\tau_{ren} \approx \tau_0 N^3 / N_e \tag{14}$$

$$\eta_0 \approx \frac{\rho R T \emptyset N^3}{M_e N_e} \tau_0 \approx G_0 \tau_0 \frac{N^3}{N_e} \approx G_0 \tau_{rep}$$
 [15]

Zero shear viscosities plotted as a function of  $N_{avg}$  (Figure 8) show a scaling of  $\eta_o \sim N^{3.10}$ , slightly more than the  $N^3$  predicted. A scaling of  $N^{3.4}$  is usually observed for entangled polymers. The slightly lower scaling may come from a population of unentangled polymers in each fraction.  $\eta_o$ , estimated from Equation 15, which is an approximation without prefactors, I is also listed in Table 5 and is in rough agreement with experiment. In a previous work using a polycarboxylate, I aph sensitive polyanion, we had obtained a puzzling scaling of  $\eta_o \sim N^{5.4}$ , one of the motivations for the present work. It is possible that the rapid protonation/deprotonation of the carboxylate repeat units provides another channel for disengaging Pol+Pol- pairs. This might explain why carboxylate PECs are usually liquid-like.

At sufficiently high temperatures all the dynamics in a polymer chain follow Arrhenius behavior,  $In\omega \sim 1/T$ , reflected in a linear  $Ina_T$  versus 1/T plot. Under these conditions, the fastest relaxation in the LVR in Figure 6 and Table 5,  $\tau_0$ , should be that of a Kuhn length. In the current system, Arrhenius response was only observed at temperatures > 50 °C (Figure S8). To correct the response to what it would have been if  $\tau_0$  were measured in the Arrhenius region (it would be faster) the measured value of  $\tau_0$  is corrected by the factor shown on the graph in Figure S8, which is a factor of about 0.71. An average  $\tau_0$  of 4.7 x  $10^{-4}$  s was read from Figure 6 which yields a corrected  $\tau_0$  of 3.3 x  $10^{-4}$  s. This is orders of magnitude slower than the Kuhn length relaxation time in neutral melts and explains the high viscosity of liquid-like coacervates, even though the polymer volume fraction is decreased significantly by the presence of water.

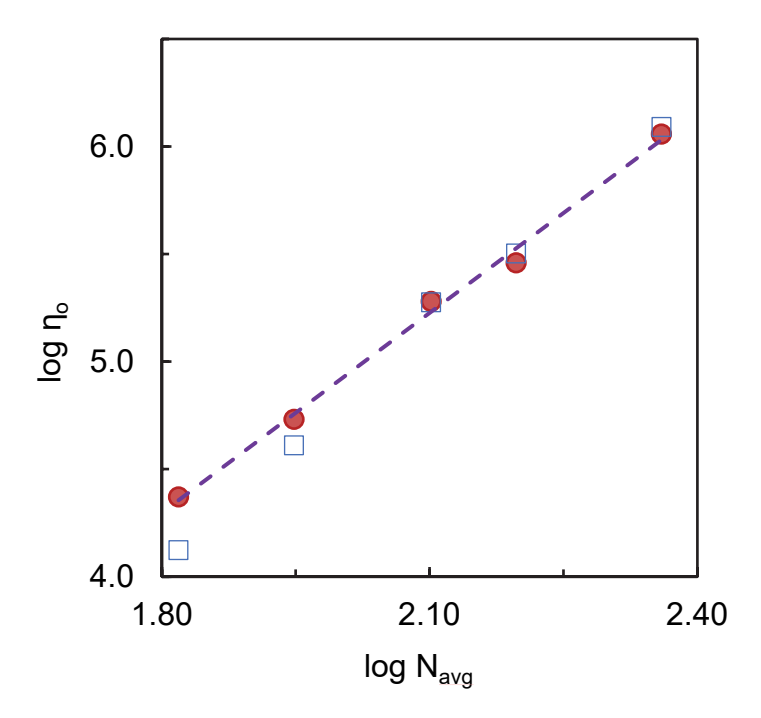


**Figure 8**. Experimental zero-shear viscosity ( $\bullet$ , see Figure S10) as a function of chain length for entangled PECs in 0.01 M NaSCN.  $T_{ref}$  = 25  $^{\circ}$ C. The measured  $\eta_0$  scales as  $\sim N^{3.10}$  (solid line). Approximate prediction  $\eta_0 \approx G_0 \tau_{rep}$  is shown by the open squares.

Breaking Charge Pairs via Doping. The experimental variables in the LVR of PECs are often interrelated by attempts at superposition, <sup>29</sup> such as TTS discussed previously. LVR at various [NaSCN]<sub>s</sub> was shifted to produce the master curve shown in Figure 9. The influence of salt was originally <sup>75</sup> attributed to the control of the lifetime of Pol+Pol- interactions by electrostatic screening. The pair lifetime,  $\tau_{pair}$  was proposed to scale with [NaCl]<sup>0.5</sup> as follows <sup>17</sup>

$$\ln \tau_{pair} \sim -A\sqrt{[salt]} + B$$
 [16]

where A and B are constants. Figure 5 shows this lifetime changes very little with added Na SCN. Equation 16 assumes the Debye-Hückel approximation to describe electrostatic shielding, in spite of the fact that PECs already contains > 1 M charges from the polyelectrolyte units themselves. Also, the authors assumed  $\phi$  did not change with [salt]. A viscoelasticity study of a more glassy PEC also employed Equation 16 and found an appropriate salt scaling if  $\phi$  was assumed to decrease with increasing salt concentration. However, in another study on length-matched polypeptides, Marciel et al. Were unable to find the scaling of Eq. 16, and instead found the dynamics (reported by the shift factor  $a_s$ ) to vary as  $e^{-[NaCl]}$ , similar to the response observed here.

Attempts at time-salt superposition often produce imperfectly-overlapping datasets,  $^{29}$  as seen in Figure 9 in the 1 – 10 rad s<sup>-1</sup> frequency range. (See also Figure 9 in reference 25, Figure

4 in reference 7, and Figure 8 in reference 40). This is because there are at least three variables – change in polymer volume fraction from swelling (which changes  $G_0$  and  $N_e$ ), lifetime of Pol<sup>+</sup>Pol<sup>-</sup>pairs, and number density of pairs - that are not sufficiently captured by two shift factors. In contrast to Equation 16, the pair lifetime changes very little over the entire [salt] range (see Figure 5B).

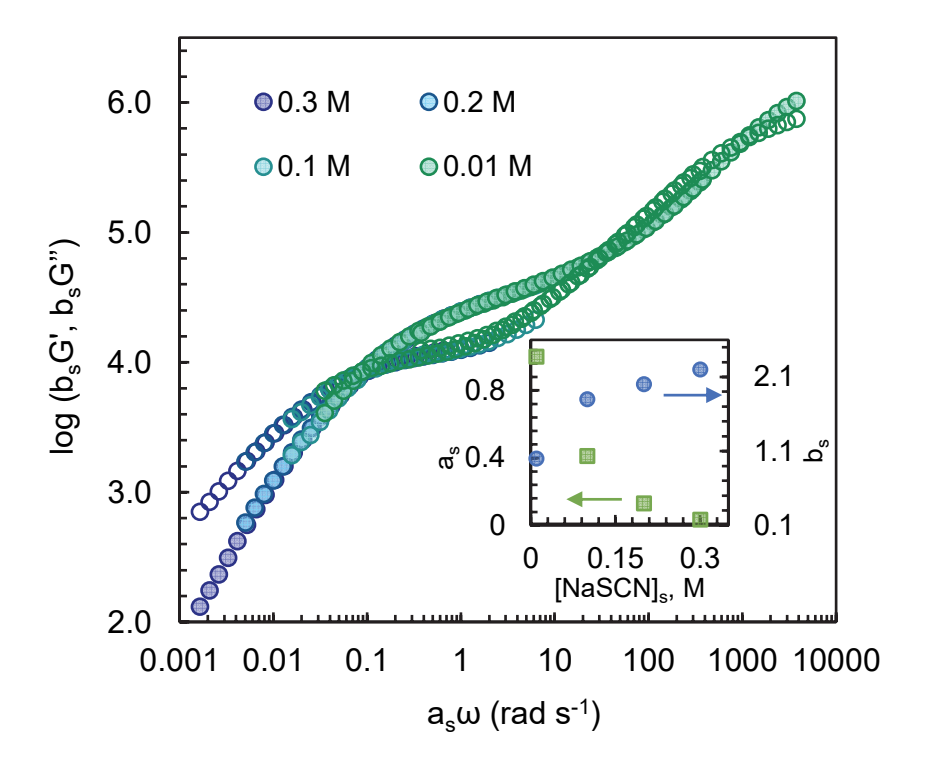


**Figure 9.** Time-salt superposition of P1479 doped with 0.01, 0.1, 0.2 and 0.3 M NaSCN at T = 25  $^{\circ}$ C. Reference salt concentration is 0.01 M. Inset shows salt shift factors  $a_{S}$  and  $b_{S}$ . See Supporting Information Figure S11 for individual time-temperature superposition data.

The viscosity was measured as a function of [NaSCN]<sub>s</sub>. At higher [MA], up to the CSC, the ions continue to exclusively break Pol<sup>+</sup>Pol<sup>-</sup>, decreasing the pair density in the complex. This is paralleled by a decrease in PEC viscosity. Figure 10 gives the zero-shear viscosity measured in P1479 as a function of *y*. Figure 10 reveals a leveling of viscosity at the lowest values of *y*, believed to be a consequence of small nonstoichiometry thus residual ions. The change in viscosity with salt concentration less pronounced than that observed in PDADMA/PSS<sup>34</sup> <sup>30</sup> <sup>76</sup>, a PEC with a glass transition temperature of 34 °C, because added salt also decreases T<sub>g</sub>. <sup>25</sup>

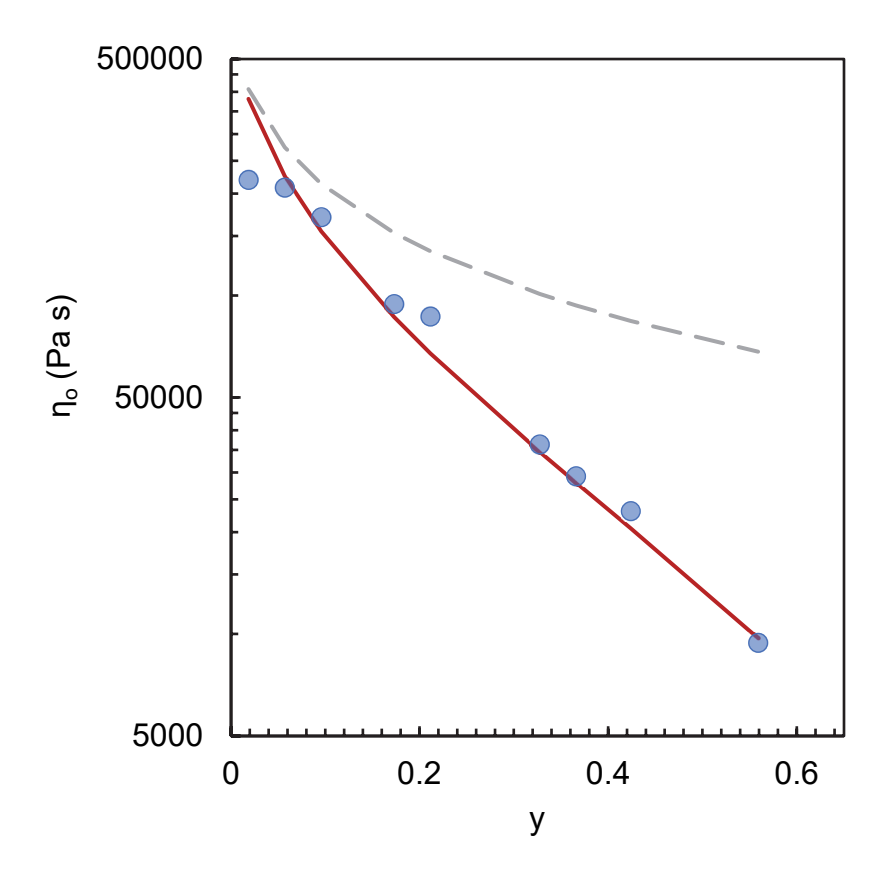


**Figure 10.** Zero shear viscosity of P1479 as a function of y (from Figure 3B) the fraction of Pol<sup>+</sup>Pol<sup>-</sup> pairs broken, at T<sub>ref</sub> = 25 °C. Viscosities were measured at T = 55 °C (see Supporting Information Figure S10B) and shifted to 25 °C using a shift factor  $a_T = 1/0.17$ . Solid line is Equation 17 with intercept fit of 5 x 10<sup>5</sup> Pa s. Dashed line shows the contribution to  $η_0$  from the decreasing polymer volume fraction  $\phi$  only.

The number of Kuhn length stickers F in Equation 13 is now (1-y)N. In a  $\theta$ -solvent for entangled polymers,  $\eta_0 \sim \phi^{4.7}$ , thus the estimated viscosity of the doped PEC,  $\eta_{0,d}$ , relative to undoped,  $\eta_{0,u}$ , is

$$\eta_{0,d} = \eta_{0,u} \frac{\tau_{0,d}}{\tau_{0,u}} \left(\frac{\phi_d}{\phi_u}\right)^{4.7} (1 - y)^2$$
 [17]

The volume fractions come from Table S2, the ratio  $\tau_{0,d}/\tau_{0,u}$  for undoped and doped PEC from Figure 5B, and y is taken from Figure 3B ( $y = r = 1.93[\text{NaSCN}]_s - 0.02$ ). Because the viscosity remains constant at low y, about 2.2 x 10<sup>5</sup> Pa s, a fit value of 5 x 10<sup>5</sup> Pa s was used as  $\eta_{0,u}$  for completely undoped PEC. Equation 17 provides a reasonable fit to most of the data. The decrease in viscosity on doping comes largely from the loss of Pol<sup>+</sup>Pol<sup>-</sup> pairs. The dotted line

shows the contribution from the decrease in volume fraction  $\left(\frac{\phi_d}{\phi_u}\right)^{4.7}$ . The  $\eta_0$  at low y coincides with a significant change in  $\phi$  over this region, which is unexpected. Though the cause is presently uncertain, this swelling is thought to be due to residual ions and the osmotic pressure of the PEC matrix.

## **Conclusions**

A decade of studies in the field have pointed to unique aspects of dynamics within PECs, but full picture of how dynamics at the monomer scale translate to bulk viscoelastic response in PECs has been slow to emerge. The current work has systematically isolated, controlled and measured the variables needed to provide a quantitative understanding of dynamics in a liquid-like polyelectrolyte coacervate. The dynamics of PECs close to, or below,  $T_g$  will be additionally slowed by cooperativity known to operate in glassy systems approaching  $T_g$ .

Although individual Pol<sup>+</sup>Pol<sup>-</sup> dynamics are fast, sticky interactions for undoped PECs act pairwise, via a pair exchange mechanism, responsible for slowing chain motion by orders of magnitude compared to neutral polymers. A Kuhn length "monomer" relaxation time of about 0.3 ms at 25 °C was measured. The dynamics of any PEC will depend critically on  $\tau_0$  and its temperature response. Variations in these parameters probably account for the wide variation of LVR observed for different combinations of Pol<sup>+</sup> and Pol<sup>-</sup>.

The use of thiocyanate ion in salt doping has enabled a breakthrough in identifying how many Pol<sup>+</sup>Pol<sup>-</sup> pairs are broken. SCN<sup>-</sup> specifically interacts with positive polymer repeat units, ensuring that one added salt breaks one Pol<sup>+</sup>Pol<sup>-</sup> pair in a site-specific PEC doping model. This specific association of a counterion within a PEC was directly demonstrated, for the first time, using the position of the CN stretching band in FTIR. The viscosity of undoped PECs scaled with N<sup>3.1</sup> in line with the sticky reptation model. A relationship for the viscosity of doped PEC was tested using NaSCN as a doping salt. Most of the decrease in viscosity on doping stems from the loss of sticky interactions and not from a modification of the Pol<sup>+</sup>Pol<sup>-</sup> pair lifetime, as originally proposed.

While every effort was made here to eliminate variables such as the pH-dependence of charge, supplemental H-bonding, polydispersity, mixed functionality, charges separated by neutral units, hydrophobic effects, and nonlinear architecture, some or all of these variables are present in most coacervating systems, especially biological ones. The formation and properties of PECs made from more complex systems remain of great interest.

# **Supporting Information**

Procedure for radiolabeling ions in PECs; procedure and size exclusion chromatography of polyelectrolytes; isothermal calorimetry method; synthesis of deuterated monomers and polymers; <sup>1</sup>H NMR of polyelectrolytes and PEC; SANS of PEC at different temperatures; critical salt concentration of wide molecular weight distribution PEC; isothermal calorimetry of PMAPTA(SCN) and PAMPS; compositions of PECs at various [NaSCN]<sub>s</sub>; time temperature

superposition of PEC pairs; shift factors for TTS; Arrhenius plot of shift factors; estimating the critical number of repeat units for entanglement; viscosity of PEC at low shear rates; TTS for PEC in various [NaSCN]<sub>s</sub>; TTS of complex viscosity of PEC pairs.

## **Notes**

The authors declare no competing financial interest.

# Acknowledgment

This research used resources at the Spallation Neutron Source, a DOE Office of Science User Facility operated by the Oak Ridge National Laboratory. This research was supported in part by the National Science Foundation, Grant DMR 2103703.

## References

- 1. Chen, Y.; Yang, M.; Schlenoff, J. B., Glass Transitions in Hydrated Polyelectrolyte Complexes. *Macromolecules* **2021**, *54*, 3822-3831.
- 2. Bungenberg de Jong, H. G.; Kruyt, H. R., Coacervation (Partial Miscibility in Colloid Systems). *Proc. Sect. Sci. K. Ned. Akad. Wetenschappen* **1929**, *32*, 849-856.
- 3. Rubinstein, M.; Colby, R. H., *Polymer Physics*. Oxford University Press: New York, 2003.
- 4. Rosales, A. M.; Anseth, K. S., The Design of Reversible Hydrogels to Capture Extracellular Matrix Dynamics. *Nat Rev Mater* **2016**, *1*, 15012.
- 5. Winne, J. M.; Leibler, L.; Du Prez, F. E., Dynamic Covalent Chemistry in Polymer Networks: A Mechanistic Perspective. *Polymer Chemistry* **2019**, *10*, 6091-6108.
- 6. Voorhaar, L.; Hoogenboom, R., Supramolecular Polymer Networks: Hydrogels and Bulk Materials. *Chem Soc Rev* **2016**, *45*, 4013-4031.
- 7. Schaaf, P.; Schlenoff, J. B., Saloplastics: Processing Compact Polyelectrolyte Complexes. *Advanced Materials* **2015**, *27*, 2420-2432.
- 8. Shamoun, R. F.; Reisch, A.; Schlenoff, J. B., Extruded Saloplastic Polyelectrolyte Complexes. *Advanced Functional Materials* **2012**, *22*, 1923-1931.
- 9. Kelly, K. D.; Schlenoff, J. B., Spin-Coated Polyelectrolyte Coacervate Films. *ACS Applied Materials & Interfaces* **2015**, *7*, 13980-13986.
- 10. Haile, M.; Sarwar, O.; Henderson, R.; Smith, R.; Grunlan, J. C., Polyelectrolyte Coacervates Deposited as High Gas Barrier Thin Films. *Macromolecular Rapid Communications* **2017**, *38*, 1600594.
- 11. Gai, M.; Li, W.; Frueh, J.; Sukhorukov, G. B., Polylactic Acid Sealed Polyelectrolyte Complex Microcontainers for Controlled Encapsulation and NIR-Laser Based Release of Cargo. *Colloids and Surfaces B: Biointerfaces* **2019**, *173*, 521-528.
- 12. Duan, Y.; Wang, C.; Zhao, M.; Vogt, B. D.; Zacharia, N. S., Mechanical Properties of Bulk Graphene Oxide/Poly(Acrylic Acid)/Poly(Ethylenimine) Ternary Polyelectrolyte Complex. *Soft Matter* **2018**, *14*, 4396-4403.
- 13. Meng, X.; Perry, S. L.; Schiffman, J. D., Complex Coacervation: Chemically Stable Fibers Electrospun from Aqueous Polyelectrolyte Solutions. *ACS Macro Letters* **2017**, *6*, 505-511.

- 14. Katchalsky, A.; Künzle, O.; Kuhn, W., Behavior of Polyvalent Polymeric Ions in Solution. *Journal of Polymer Science* **1950,** *5*, 283-300.
- 15. Muthukumar, M., 50th Anniversary Perspective: A Perspective on Polyelectrolyte Solutions. *Macromolecules* **2017**, *50*, 9528-9560.
- 16. Overbeek, J. T. G.; Voorn, M. J., Phase Separation in Polyelectrolyte Solutions. Theory of Complex Coacervation. *Journal of Cellular and Comparative Physiology* **1957**, *49*, 7-26.
- 17. Spruijt, E.; Cohen Stuart, M. A.; van der Gucht, J., Linear Viscoelasticity of Polyelectrolyte Complex Coacervates. *Macromolecules* **2013**, *46*, 1633-1641.
- 18. Schindler, T.; Nordmeier, E., The Stability of Polyelectrolyte Complexes of Calf-Thymus DNA and Synthetic Polycations: Theoretical and Experimental Investigations. *Macromol Chem Physic* **1997**, *198*, 1943-1972.
- 19. Schlenoff, J. B., Site-Specific Perspective on Interactions in Polyelectrolyte Complexes: Toward Quantitative Understanding. *The Journal of Chemical Physics* **2018**, *149*, 163314.
- 20. Ghasemi, M.; Larson, R. G., Future Directions in Physiochemical Modeling of the Thermodynamics of Polyelectrolyte Coacervates. *AICHE J* **2022**, *68*, e17646.
- 21. Radhakrishna, M.; Basu, K.; Liu, Y.; Shamsi, R.; Perry, S. L.; Sing, C. E., Molecular Connectivity and Correlation Effects on Polymer Coacervation. *Macromolecules* **2017**, *50*, 3030-3037.
- 22. Rumyantsev, A. M.; Johner, A.; Tirrell, M. V.; de Pablo, J. J., Unifying Weak and Strong Charge Correlations within the Random Phase Approximation: Polyampholytes of Various Sequences. *Macromolecules* **2022**, *55*, 6260-6274.
- 23. Yang, M.; Digby, Z. A.; Schlenoff, J. B., Precision Doping of Polyelectrolyte Complexes: Insight on the Role of Ions. *Macromolecules* **2020**, *53*, 5465-5474.
- 24. Ghasemi, M.; Friedowitz, S.; Larson, R. G., Analysis of Partitioning of Salt through Doping of Polyelectrolyte Complex Coacervates. *Macromolecules* **2020**, *53*, 6928-6945.
- 25. Shamoun, R. F.; Hariri, H. H.; Ghostine, R. A.; Schlenoff, J. B., Thermal Transformations in Extruded Saloplastic Polyelectrolyte Complexes. *Macromolecules* **2012**, *45*, 9759-9767.
- 26. Liu, Y. L.; Winter, H. H.; Perry, S. L., Linear Viscoelasticity of Complex Coacervates. *Adv Colloid Interfac* **2017**, *239*, 46-60.
- 27. Hamad, F. G.; Chen, Q.; Colby, R. H., Linear Viscoelasticity and Swelling of Polyelectrolyte Complex Coacervates. *Macromolecules* **2018**, *51*, 5547-5555.
- 28. Huang, J.; Morin, F. J.; Laaser, J. E., Charge-Density-Dominated Phase Behavior and Viscoelasticity of Polyelectrolyte Complex Coacervates. *Macromolecules* **2019**, *52*, 4957-4967.
- 29. Larson, R. G.; Liu, Y.; Li, H., Linear Viscoelasticity and Time-Temperature-Salt and Other Superpositions in Polyelectrolyte Coacervates. *Journal of Rheology* **2021**, *65*, 77-102.
- 30. Ali, S.; Prabhu, V., Relaxation Behavior by Time-Salt and Time-Temperature Superpositions of Polyelectrolyte Complexes from Coacervate to Precipitate. *Gels* **2018**, *4*, 11.
- 31. Yang, M.; Shi, J.; Schlenoff, J. B., Control of Dynamics in Polyelectrolyte Complexes by Temperature and Salt. *Macromolecules* **2019**, *52*, 1930-1941.
- 32. Spruijt, E.; Westphal, A. H.; Borst, J. W.; Cohen Stuart, M. A.; van der Gucht, J., Binodal Compositions of Polyelectrolyte Complexes. *Macromolecules* **2010**, *43*, 6476-6484.
- 33. Li, L.; Srivastava, S.; Andreev, M.; Marciel, A. B.; de Pablo, J. J.; Tirrell, M. V., Phase Behavior and Salt Partitioning in Polyelectrolyte Complex Coacervates. *Macromolecules* **2018**, *51*, 2988-2995.

- 34. Wang, Q. F.; Schlenoff, J. B., The Polyelectrolyte Complex/Coacervate Continuum. *Macromolecules* **2014**, *47*, 3108-3116.
- 35. Syed, V. M. S.; Srivastava, S., Time–Ionic Strength Superposition: A Unified Description of Chain Relaxation Dynamics in Polyelectrolyte Complexes. *ACS Macro Letters* **2020**, *9*, 1067-1073.
- 36. Marciel, A. B.; Srivastava, S.; Tirrell, M. V., Structure and Rheology of Polyelectrolyte Complex Coacervates. *Soft Matter* **2018**, *14*, 2454-2464.
- 37. Rubinstein, M.; Semenov, A. N., Dynamics of Entangled Solutions of Associating Polymers. *Macromolecules* **2001**, *34*, 1058-1068.
- 38. Zhang, Z.; Chen, Q.; Colby, R. H., Dynamics of Associative Polymers. *Soft Matter* **2018**, *14*, 2961-2977.
- 39. Leibler, L.; Rubinstein, M.; Colby, R. H., Dynamics of Reversible Networks. *Macromolecules* **1991**, 24, 4701-4707.
- 40. Akkaoui, K.; Yang, M.; Digby, Z. A.; Schlenoff, J. B., Ultraviscosity in Entangled Polyelectrolyte Complexes and Coacervates. *Macromolecules* **2020**, *53*, 4234-4246.
- 41. Digby, Z. A.; Yang, M.; Lteif, S.; Schlenoff, J. B., Salt Resistance as a Measure of the Strength of Polyelectrolyte Complexation. *Macromolecules* **2022**, *55*, 978-988.
- 42. Tsuchida, E.; Osada, Y.; Abe, K., Formation of Polyion Complexes between Polycarboxylic Acids and Polycations Carrying Charges in the Chain Backbone. *Die Makromolekulare Chemie* **1974**, *175*, 583-592.
- 43. Salehi, A.; Larson, R. G., A Molecular Thermodynamic Model of Complexation in Mixtures of Oppositely Charged Polyelectrolytes with Explicit Account of Charge Association/Dissociation. *Macromolecules* **2016**, *49*, 9706-9719.
- 44. Fisher, R. S.; Elbaum-Garfinkle, S., Tunable Multiphase Dynamics of Arginine and Lysine Liquid Condensates. *Nat Commun* **2020**, *11*, 4628.
- 45. Digby, Z. A.; Chen, Y.; Akkaoui, K.; Schlenoff, J. B., Bulk Biopolyelectrolyte Complexes from Homopolypeptides: Solid "Salt Bridges". *Biomacromolecules* **2023**, *24*, 1453-1462.
- 46. Perry, S. L.; Leon, L.; Hoffmann, K. Q.; Kade, M. J.; Priftis, D.; Black, K. A.; Wong, D.; Klein, R. A.; Pierce, C. F.; Margossian, K. O.; Whitmer, J. K.; Qin, J.; de Pablo, J. J.; Tirrell, M., Chirality-Selected Phase Behaviour in Ionic Polypeptide Complexes. *Nat Commun* **2015**, *6*, 6052.
- 47. Gummel, J.; Cousin, F.; Boué, F., Structure Transition in PSS/Lysozyme Complexes: A Chain-Conformation-Driven Process, as Directly Seen by Small Angle Neutron Scattering. *Macromolecules* **2008**, *41*, 2898-2907.
- 48. Fisher, L. W.; Sochor, A. R.; Tan, J. S., Chain Characteristics of Poly(2-Acrylamido-2-Methylpropanesulfonate) Polymers. 2. Comparison of Unperturbed Dimensions and Persistence Lengths. *Macromolecules* **1977**, *10*, 955-959.
- 49. Trinh, C. K.; Schnabel, W., Ionic-Strength Dependence of the Stability of Polyelectrolyte Complexes Its Importance for the Isolation of Multiply-Charged Polymers. *Angew Makromol Chem* **1993**, *212*, 167-179.
- 50. Bungenberg de Jong, H. G., In Colloid Science, Kruyt, H. R., Ed. Elsevier: Amsterdam, 1949; Vol. 2.
- 51. Schlenoff, J. B.; Yang, M.; Digby, Z. A.; Wang, Q., Ion Content of Polyelectrolyte Complex Coacervates and the Donnan Equilibrium. *Macromolecules* **2019**, *52*, 9149-9159.

- 52. Mongcopa, K. I. S.; Tyagi, M.; Mailoa, J. P.; Samsonidze, G.; Kozinsky, B.; Mullin, S. A.; Gribble, D. A.; Watanabe, H.; Balsara, N. P., Relationship between Segmental Dynamics Measured by Quasi-Elastic Neutron Scattering and Conductivity in Polymer Electrolytes. *ACS Macro Letters* **2018**, *7*, 504-508.
- 53. Crank, J., *The Mathematics of Diffusion*. Clarendon Press: Oxford, 1975.
- 54. Helfferich, F. G., *Ion Exchange*. McGraw-Hill: New York,, 1962; p 624 p.
- 55. Schönemann, E.; Laschewsky, A.; Rosenhahn, A., Exploring the Long-Term Hydrolytic Behavior of Zwitterionic Polymethacrylates and Polymethacrylamides. *Polymers* **2018**, *10*, 639.
- 56. Spruijt, E.; Leermakers, F. A. M.; Fokkink, R.; Schweins, R.; van Well, A. A.; Cohen Stuart, M. A.; van der Gucht, J., Structure and Dynamics of Polyelectrolyte Complex Coacervates Studied by Scattering of Neutrons, X-Rays, and Light. *Macromolecules* **2013**, *46*, 4596-4605.
- 57. Chen, Y.; Yang, M.; Shaheen, S. A.; Schlenoff, J. B., Influence of Nonstoichiometry on the Viscoelastic Properties of a Polyelectrolyte Complex. *Macromolecules* **2021**, *54*, 7890-7899.
- 58. Markarian, M. Z.; Hariri, H. H.; Reisch, A.; Urban, V. S.; Schlenoff, J. B., A Small-Angle Neutron Scattering Study of the Equilibrium Conformation of Polyelectrolytes in Stoichiometric Saloplastic Polyelectrolyte Complexes. *Macromolecules* **2012**, *45*, 1016-1024.
- 59. Fares, H. M.; Ghoussoub, Y. E.; Delgado, J. D.; Fu, J.; Urban, V. S.; Schlenoff, J. B., Scattering Neutrons Along the Polyelectrolyte Complex/Coacervate Continuum. *Macromolecules* **2018**, *51*, 4945-4955.
- 60. Kuzminskaya, O.; Riemer, S.; Dalgliesh, R.; Almásy, L.; Hoffmann, I.; Gradzielski, M., Structure and Phase Behavior of Interpolyelectrolyte Complexes of PDADMAC and Hydrophobically Modified PAA (HM-PAA). *Macromol Chem Physic* **2023**, *224*, 2200276.
- 61. Liu, X.; Chapel, J.-P.; Schatz, C., Structure, Thermodynamic and Kinetic Signatures of a Synthetic Polyelectrolyte Coacervating System. *Adv Colloid Interfac* **2017**, *239*, 178-186.
- 62. Zirkel, A.; Richter, D.; Fetters, L. J.; Schneider, D.; Graciano, V.; Hadjichristidis, N., A SANS-Based Evaluation of the Chain Dimension Temperature Dependence of Poly(Ethylethylene) Under .Theta.-Conditions. *Macromolecules* **1995**, *28*, 5262-5266.
- 63. Ghostine, R. A.; Shamoun, R. F.; Schlenoff, J. B., Doping and Diffusion in an Extruded Saloplastic Polyelectrolyte Complex. *Macromolecules* **2013**, *46*, 4089-4094.
- 64. Mehan, S.; Herrmann, L.; Chapel, J.-P.; Jestin, J.; Berret, J.-F.; Cousin, F., The Desalting/Salting Pathway: A Route to Form Metastable Aggregates with Tuneable Morphologies and Lifetimes. *Soft Matter* **2021**, *17*, 8496-8505.
- 65. Ma, Y.; Ali, S.; Prabhu, V. M., Enhanced Concentration Fluctuations in Model Polyelectrolyte Coacervate Mixtures Along a Salt Isopleth Phase Diagram. *Macromolecules* **2021**, *54*, 11338-11350.
- 66. Lounis, F. M.; Chamieh, J.; Leclercq, L.; Gonzalez, P.; Geneste, A.; Prelot, B.; Cottet, H., Interactions between Oppositely Charged Polyelectrolytes by Isothermal Titration Calorimetry: Effect of Ionic Strength and Charge Density. *The Journal of Physical Chemistry B* **2017**, *121*, 2684-2694.
- 67. Zhang, P.; Wang, Z.-G., Supernatant Phase in Polyelectrolyte Complex Coacervation: Cluster Formation, Binodal, and Nucleation. *Macromolecules* **2022**, *55*, 3910-3923.
- 68. Kabanov, V. M.; Zezin, A. B., Soluble Interpolymeric Complexes as a New Class of Synthetic Polyelectrolyte. *Pure Appl. Chem.* **1984**, *56*, 343-354.

- 69. Tsuchida, E.; Osada, Y.; Sanada, K., Interaction of Poly(Styrene Sulfonate) with Polycations Carrying Charges in the Chain Backbone. *Journal of Polymer Science Part A-1: Polymer Chemistry* **1972,** *10*, 3397-3404.
- 70. Dautzenberg, H., Polyelectrolyte Complex Formation in Highly Aggregating Systems: Methodical Aspects and General Tendencies. In *Physical Chemistry of Polyelectrolytes, Surfactant Science Series, Vol. 99*, Radeva, T., Ed. Dekker: New York, 2001; pp 743 792.
- 71. Lee, H.; Choi, J.-H.; Cho, M., Vibrational Solvatochromism and Electrochromism of Cyanide, Thiocyanate, and Azide Anions in Water. *Physical Chemistry Chemical Physics* **2010**, *12*, 12658-12669.
- Adhikary, R.; Zimmermann, J.; Dawson, P. E.; Romesberg, F. E., Temperature Dependence of CN and SCN IR Absorptions Facilitates Their Interpretation and Use as Probes of Proteins. *Analytical Chemistry* **2015**, *87*, 11561-11567.
- 73. Winter, H. H., Can the Gel Point of a Cross-Linking Polymer Be Detected by the G' G" Crossover? *Polymer Engineering & Science* **1987**, *27*, 1698-1702.
- 74. Fetters, L. J.; Lohse, D. J.; Richter, D.; Witten, T. A.; Zirkel, A., Connection between Polymer Molecular Weight, Density, Chain Dimensions, and Melt Viscoelastic Properties. *Macromolecules* **1994**, *27*, 4639-4647.
- 75. Spruijt, E.; Sprakel, J.; Lemmers, M.; Stuart, M. A. C.; van der Gucht, J., Relaxation Dynamics at Different Time Scales in Electrostatic Complexes: Time-Salt Superposition. *Physical Review Letters* **2010**, *105*, 208301.
- 76. Liu, Y.; Momani, B.; Winter, H. H.; Perry, S. L., Rheological Characterization of Liquid-to-Solid Transitions in Bulk Polyelectrolyte Complexes. *Soft Matter* **2017**, *13*, 7332-7340.